Chapter 2

Arginine and lysine clustering on calix[4]arene macrocycles as novel strategy for improving gene delivery

2.1 Introduction

The ability to cross the plasma membrane and gain access to the cell interior is the basic requirement and also the major problem in any intracellular drug- or gene-delivery protocol.

Biology has developed different ways to circumvent these obstacles, thanks to some proteins able to permeate mammalian cell membranes. The localized region in the protein known as the protein transduction domain (PTD) confers this ability, and these peptide sequences are commonly named cell penetrating peptides (CPPs) or Trojan Horse peptides.[1] During the past two decades, considerable research has focused on the development of CPPs, with the aim of making possible the intracellular delivery of bioactive molecules with intrinsically low membrane permeability.[2] In particular, after the discovery that an arginine-rich segment of Transactivator of Transcription (TAT) of the Human Immunodeficiency Virus can enter cells efficiently, either alone[3] or linked to macromolecules,[4] it became the most widely studied prototypical example. It opened the door to deep investigations about biological activity of similarly structured arginine-rich peptides[5] and to synthesis of novel intracellular delivery vectors composed only of arginine.[6]

Recent developments in molecular biology and genome science have led to identify a number of disease-related genes. Attempts to apply these findings to the development of therapies for genetic and acquired diseases are in progress. So, thanks to their high internalization ability CPPs have received attention as attractive candidates for Nucleic Acid Pharmaceuticals (NAP) delivery (genes, plasmids, short oligonucleotides and small interfering RNA).[7]

There are two fundamental types of CPPs that have been utilized for intracellular delivery of therapeutic molecules, including NAPs: 1) cationic CPPs, which are short peptides mainly composed of arginine, lysine and histidine. These amino acids are responsible for the cationic charge of the peptide that will mediate the interaction with anionic motifs on the plasma membrane; 2) amphiphilic peptides, which have lipophilic and hydrophilic tails are responsible for mediating the peptide translocation across the plasma membrane.

The common feature of most of CPPs is the high density of basic amino acid residues. Whereas both arginine and lysine are representative basic amino acids, oligoarginines generally have a higher internalization efficiency compared with oligolysines possessing the same number of residues.[8] Arginine side group is a stronger base (pKa of the

guanidinium ion: ~12.5) than lysine (pKa of the ε-ammonium ion: ~10.5). Its guanidinium moiety may form two hydrogen bonds with phosphate, sulfate, and carboxylate in cell-membrane-associated molecules (e.g., lipids and glycosaminoglycans) (**Fig 2.1**), whereas lysine can form only one hydrogen bond with these groups.[9]

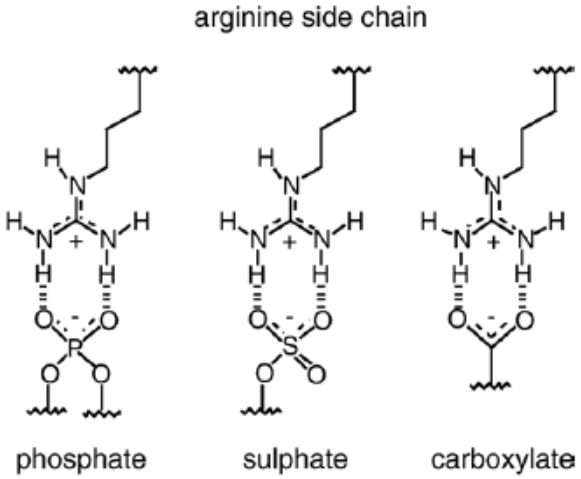

Fig 2.1 Hydrogen bonds can be formed by side chain guanidino moiety of arginine with phosphates, sulfates and carboxylates.

On the basis of all these factors, among the membrane-permeable peptide vectors, those rich in arginines are frequently employed.

Although transfection of plasmid DNAs (pDNAs) into cells in complexes with TAT itself or other unmodified CPPs is well know in literature, the delivery was not as efficient as in case of cationic liposomes (e.g. Lipofectamine-LTX) or polymers (e.g. polyethyleneimine-PEI).[4a,10]

To improve transfection efficiency, several studies evaluated the effect of the insertion of a hydrophobic portion to arginine-rich CPPs. The increased hydrophobicity of the complex may enhance cell surface adsorption and the non-electrostatic interactions in the plasmid/CPP complexes may enhance compaction of the pDNA, important aspects for the uptake.

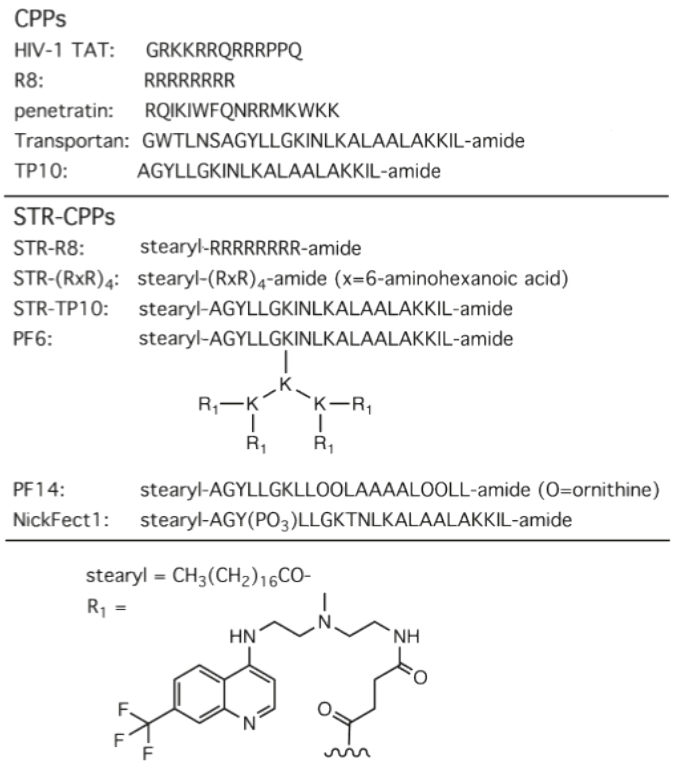

Fig 2.2 Amino acid sequences of representative CPPs and stearylated CPPs (STR-CPPs)

In a comparative study with N-terminally acylated oligoarginines having variable acyl groups and number of arginines, stearyl-octaarginine (STR-R8) was found to have the highest transfection efficiency, similar to Lipofectamine, and no significant cytotoxicity.[11] The stearyl moieties lead to the formation of self-assembled nanoparticles with a NAP-containing core-shell structures. These nanoparticles maintain a positive surface charge thus facilitating the cellular uptake.

Stearylated arginine-rich CPPs are not only useful for the compaction of NAPs; they can be easily exploited for the surface modification of liposomes, as was shown for R8-Multifunctional Enveloped-type NanoDevice (MEND).[12] The modification of liposomes with R8 was easily achieved by the addition of STR-R8 to the liposomal solution, leading to insertion of the lipophilic portion into the external hydrophobic shell. The stearyl moiety firmly anchors the peptide to the surface of the liposome while the flexibility of the peptide is maintained.[13] The study of even more sophisticated MEND concepts continues to develop rational non-viral gene delivery systems equipped with various functional devices, including ligands for specific receptors and pH-sensitive fusogenic envelopes.[14]

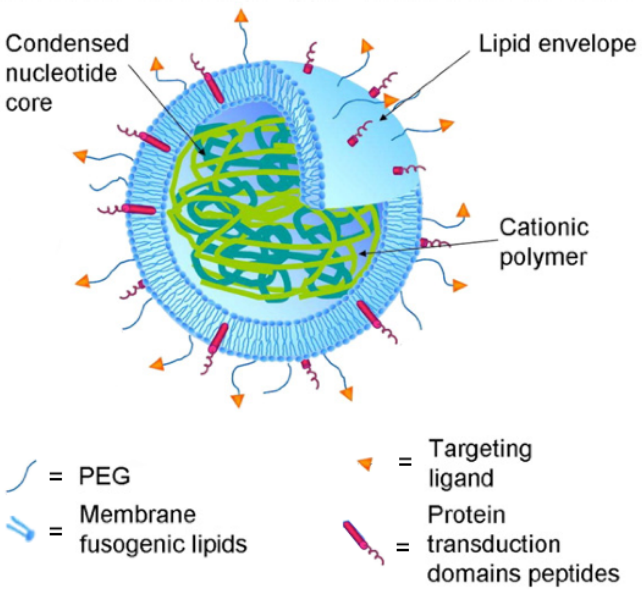

Fig 2.3 Schematic representation of multifunctional envelope-type nano-device (MEND). The MEND consists of condensed DNA molecules, coated with a lipid envelope modified with functional device such as PEG for long blood circulation, ligand for specific targeting, a protein transduction domain peptide to increase intracellular availability, and fusogenic lipids to enhance endosomal escape.[14]

Clearly, due to their peptide nature and no-buffering properties, the main drawback with the use of CPPs seems to be entrapment of peptides in endosomes following endocytosis. A series of novel, chemically modified CPPs with endosomolytic properties have then been designed for efficient delivery of NAPs. Some publications[15] have reported that TAT peptide mediated transfection in cultured cells is strongly dependent on the addition of chloroquine, a weak base that induces osmotic swelling, thus promoting the disruption of endosomal compartments. However this strategy is not practical for in vivo gene-delivery applications. Therefore, attempts have been made to utilize covalent conjugates of CPPs and amines with buffering abilities. PF6 (**Fig 2.2**), for example, was thus developed by Langel's group as a novel peptide,[16] bearing four trifluoromethylquinoline moieties connected to a lysine side chain of sequence STR-TP10 to improve endosomal escape of the peptide. Protonatable amines in PEI could be also used to replace chloroquine: in fact TAT peptide was covalently coupled to PEI, directly[17] or through a hetero-bifunctional polyethylenglycol (PEG) spacer resulting in a Tat–PEG–PEI conjugate.[8b] Both these examples represent new approaches to non-viral gene therapy, comprising protection for plasmid DNA, low toxicity and significantly enhanced transfection efficiency under in vivo conditions.

As mentioned above, the guanidinium head group is the central structural feature required for hydrogen-bond formation with cellular components and consequent peptide uptake. Thus, a number of novel vectors, bearing guanidinium moieties on various backbone structures, have been designed to emulate the cell-penetrating function of natural systems (**Fig 2.4**). These include oligoarginine peptoids that have the side chain attached to the nitrogen instead of carbon,[18] guanidinium-rich oligocarbamates[19] and polyguanidinium dendrimers.[20] Membrane-permeable oligonucleotides and peptide nucleic acids have also been investigated as scaffolds.[21] Guanidinium-rich transporters (GRTs) exhibited indeed high water solubility and were taken up into cells, sometime faster than TAT peptide.

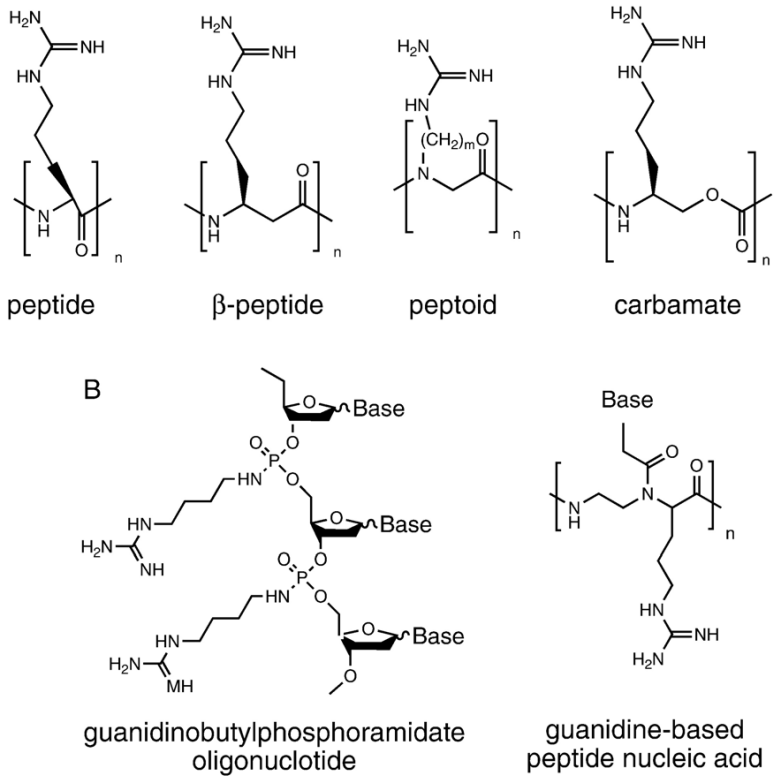

Fig 2.4 Guanidinium-rich transporters having various backbone structures.

All these examples indicate that research enthusiastically continues towards the development of vectors having even higher translocation efficiencies, lower cytotoxicity and a greater degree of selectivity to specific cells and organs.

There are only few examples in which the arginine unit was introduced in a calixarene scaffold, and none of them is finalized to gene delivery or cell penetration.

In the first example a calix[4]arene was derivatized with an RGD motif at the upper rim (**Fig 2.5**) via solid phase synthesis, to obtain a potential integrin inhibitor.[22]

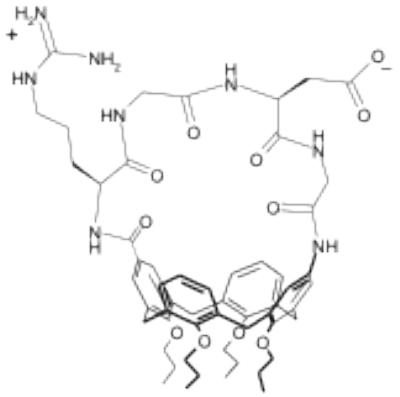

Fig 2.5 Structural formula of RGD containing calix[4]arene synthesized as a potential integrin inhibitor.

In the second example, a calix[4]arene functionalized with two N-acetyl arginine units (**Fig 2.6**) was used as stopper for [2]rotaxanes.[23] The calix[4]arene provides the necessary hydrophobic pocket for strong association in aqueous solutions, and the rotaxane ring was envisioned as a crude mimic of an antibody hypervariable loop. Acetyl-protected arginines were used as the recognition elements because they are a key residue in protein binding domains[24] and contain a chiral center that could potentially provide diastereomeric complexes with chiral guests.

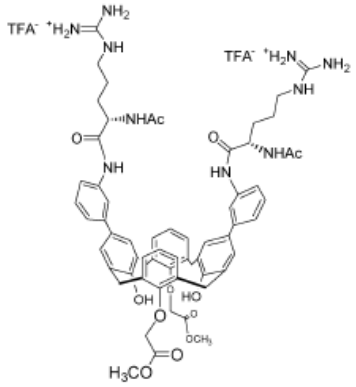

Fig 2.6 Structural formula of an arginine containing calix[4]arene studied as stopper of a [2]rotaxane

In the third example, four arginine units were directly bound to the upper rim of a calix[4]arene, *via* their α−amino groups (**Fig 2.7**) to obtain stoppers of potassium channels.[25] Potassium channels are major targets in biomedical and pharmacological research, because many diseases, mostly nervous disturbances, are linked to these membrane proteins.

The authors proposed that the conical shape of calix[4]arene scaffold is complementary to the shape of the outer vestibule of a Kv channel, while the arginine units match the negatively charged groups of the channel at the “turret loop” exposed at the extracellular surface.

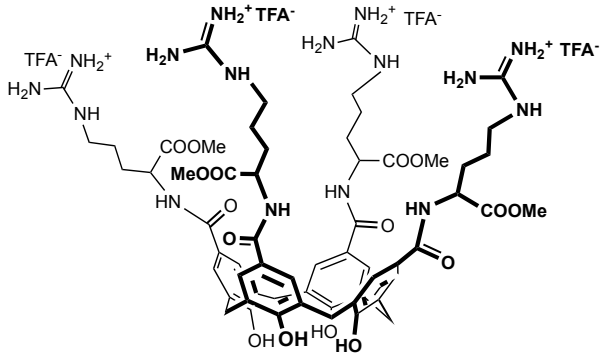

Fig 2.7 Structural formula of calix[4]arene studied as channel blockers.

Considering the CPPs properties and the previously collected positive data on transfection abilities of calixarene simply functionalized with guanidinium,[26] we turned our attention to the development of monodisperse calixarene derivatives bearing basic amino acids (arginine and lysine) as potential non-viral vectors. For our purposes, we planned the use of new arrangement respect to the natural CPPs and their already known analogues. Instead of long peptides or linear arrays of guanidinylated derivatives, we decided to explore the effects of a cyclic cluster (**Fig 2.8**). This was achieved through the connection of the amino acids to the calix[4]arene rims with resulting one to one ratio between amino acid and lipophilic tail, unlike what observed in the modified CPPs bearing multiple active units for each alkyl/acyl chain.

Furthermore, in this type of arrangement, the arginine α-amine, not involved in an amide bond formation, represents an additional charged group useful for DNA binding and a weaker base useful in a proton sponge effect to promote endosomal escape. In fact, on one hand the vector ability in buffering pH, due to the presence of amines with different basicity, contrasts the pH drop in the endosome, signal otherwise used by the cell to start the degradation of extraneous complexes. On the other hand, at the same time, a large increase in ionic concentration within endosome alters its osmolarity and facilitates the rupture and release of vector-DNA complexes into the cytoplasm.[27] The different rim

functionalization of compounds described below allowed accessing to segregated cationic and lipophilic domains for which biomimetic self-assembly and gene delivery properties could be expected ("facial amphiphilicity" concept).

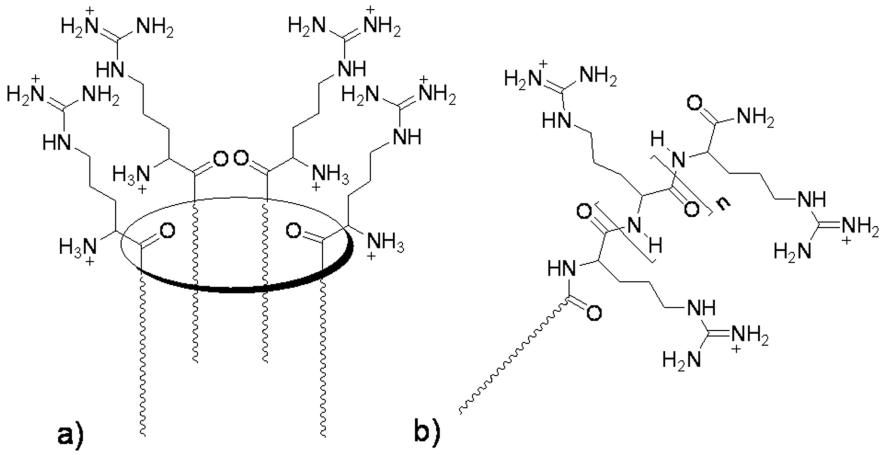

Fig 2.8 Arginine arrays. a) Cyclic *versus* b) linear array.

2.2 Results and discussion

2.2.1 Synthesis

The C-linked tetraarginino- tetrahexyloxy-calix[4]arene **3**, previously obtained in this laboratory in low yields and after purification by HPLC, in preliminary studies had shown good transfection abilities.[28] Therefore, the first aim of this PhD project has been to improve its synthesis and then to investigate in greater details its properties. In parallel, calixarene **5**, with L-lysine units instead of arginines as source of positive charge, was obtained to explore the biological properties of this amino acid when installed on a calixarene scaffold, in terms of gene delivery capability.

Additionally, inspired by good properties of the guanidino-calix[4]arene **I** as potent non-viral vector [26b,c] (**Fig 2.9**), a calixarene derivative (**11**) with L-arginine units at the lower rim was also synthesized.

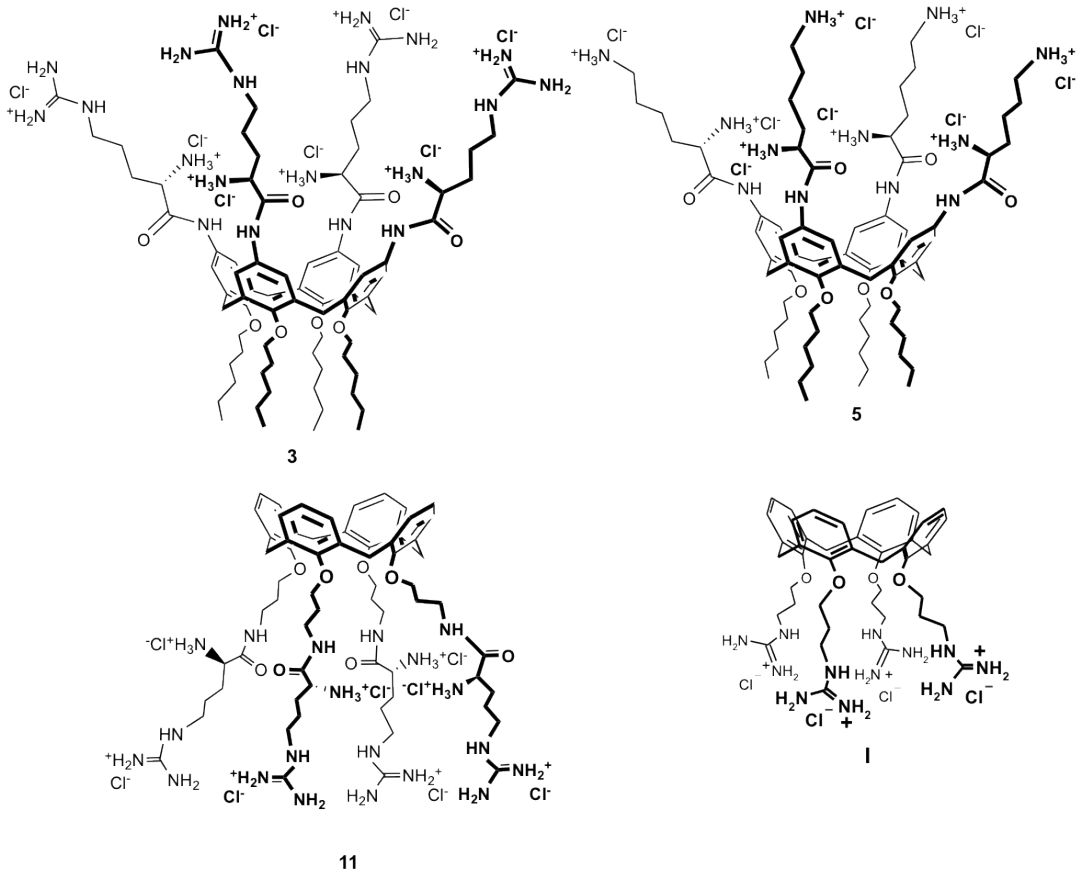

Fig 2.9 Structural formulas of peptido-calix[4]arenes **3**, **5** and **11**, and the lower rim guanidino-calix[4]arene **I**.

The general strategy adopted to synthesize these three compounds substantially consisted in two steps: the coupling of the amino acid, conveniently protected on the amino and guanidine groups, with an appropriate amino-calix[4]arene derivative, followed by deprotection. The two upper rims derivative **3** and **5** were prepared starting from tetraamino-tetrahexyloxycalix[4]arene **1**[26a]; for the synthesis of **11**, the lower rim tetrapropylamino precursor **9** was used.[31]

The success of these reactions was tightly dependent on the reactivity of these two macrocyclic intermediates (**1** and **11**) and on the nature of the protecting groups used for the amino acids.

First attempts in the coupling reactions on calixarene **1** were carried out using DCC and HOBt (Hydroxybenzotriazole) as typical coupling agents of the peptide synthesis. The removal of dicyclohexylurea (DCU) by filtration or even chromatography revealed to be a problem. Moreover, an N-acylurea by-product (**Fig 2.10**), formed through an O-acylisourea rearrangement of the active intermediate from DCC-amino acid,[29] was obtained in

substantial amount, because of the low nucleophilicity and reactivity of the aromatic amines. This slows down the desired coupling, negatively affecting the yield.

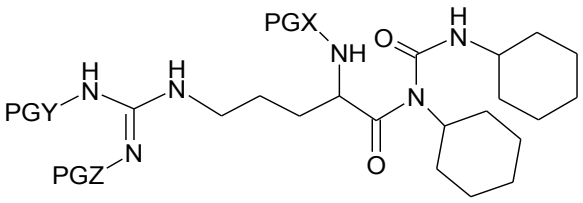

Fig 2.10 N-acylurea by-product. (PGX, PGY, PGZ = protecting groups)

Fortunately, problems in side reactions and purification were largely limited using EDC (1-ethyl-3-(3-dimethylaminopropyl)carbodiimide) and HOBt to attach Boc-L-Arg(Pbf)-OH and Boc-L-Lysine(Boc)-OH at the upper rim and the yields could be consistently increased respect to the previous procedures (**Scheme 1**).

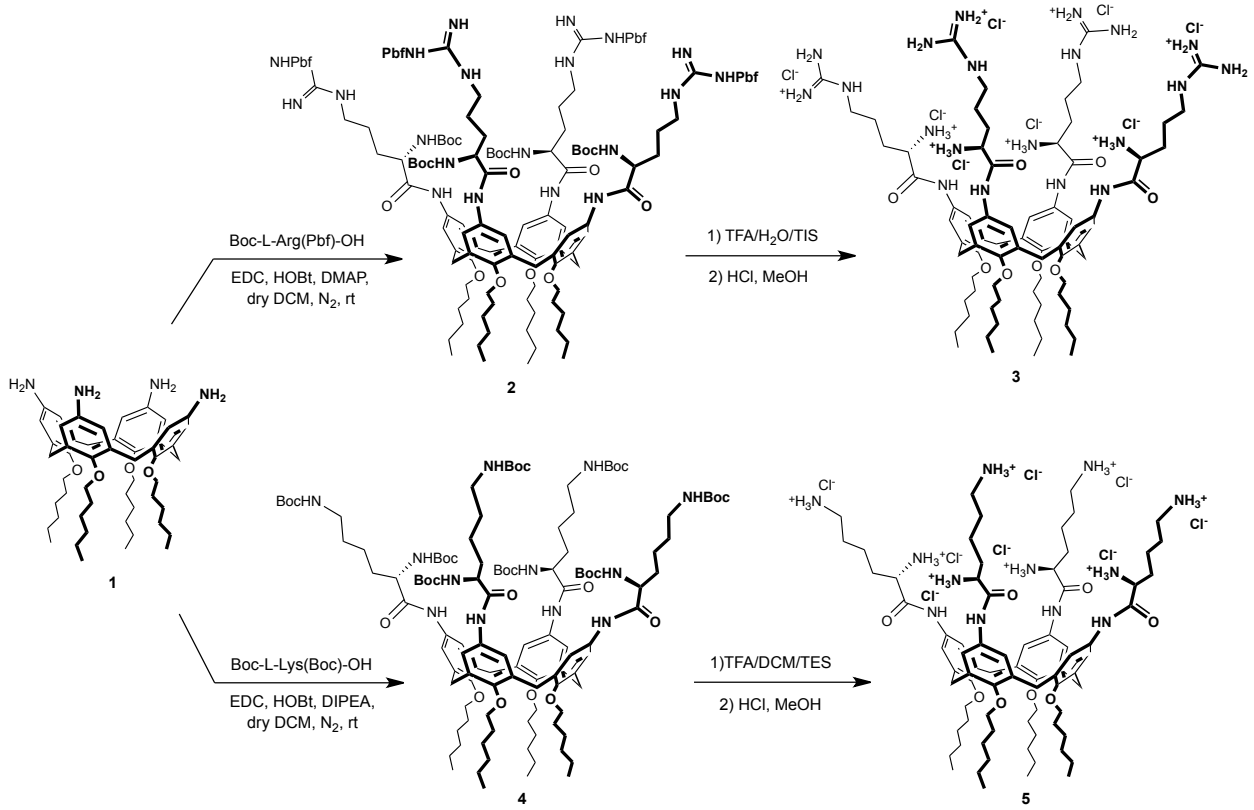

Scheme 1: synthesis of upper rim arginino-calix[4]arene **3** and lysino-calix[4]arene **5**

The removal of the protecting groups present on the amino acid units requires acid conditions. The reactions proceeded to completion in relative short time in presence of TFA solution (95% and 10% for compounds **2** and **4**, respectively) and silane as scavenger of carbocations. Then, TFA-counterion was exchanged by adding and evaporating 10mM HCl methanol solution to finally afford the target molecules **3** and **5** in quantitative yield.

Meanwhile, considering the good preliminary results in terms of biological activity obtained with calixarene **3**, an acyclic Gemini-type analogue **8** was synthesized in order to verify if the macrocyclic pre-organized structure could play an important role in DNA complexation and delivery.

Ipso-nitration reaction with $NaNO_3$ in CF_3COOH of O-alkylated derivative **6** and subsequent reduction using $NH_2NH_2 \cdot H_2O$ and a catalytic amount of Pd/C (10%) led to the amino derivative **7**, the acyclic scaffold on which the final arginino product **8** was built through a procedure similar to that used for the upper rim calix[4]arene **3** (**Scheme 2**).

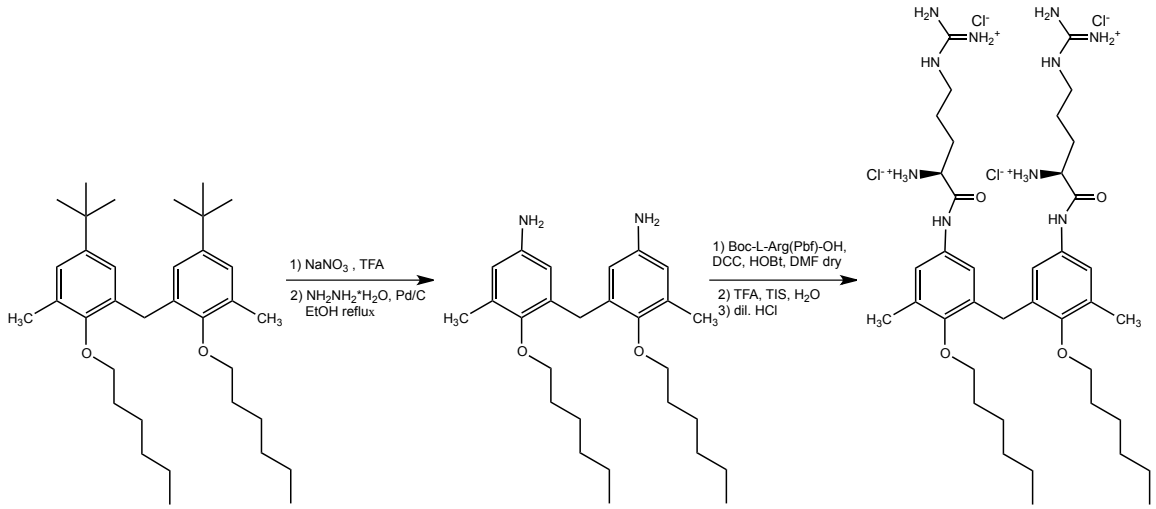

6 7 8

Scheme 2: synthesis of Gemini-type derivative **8**

For the synthesis of the lower rim arginino-calix[4]arene **11**, we had to take in account that aminopropyl derivatives of **9** resulted, in previous studies, particularly sensitive to the acidic conditions necessary to remove certain arginine protecting groups, leading to substantial decomposition of the products. Therefore, for the coupling with **9** we selected the N_α-Cbz-Arg-OH whose deprotection is performed with catalytic hydrogenation

(**Scheme 3**). The coupling product **10** was isolated in good yield; in this case, by-products (DCU and the N-acylurea rearrangement product) and excess of the monoprotected arginine were easily removed by chromatography on silica cartridges, functionalized with ammonium groups.

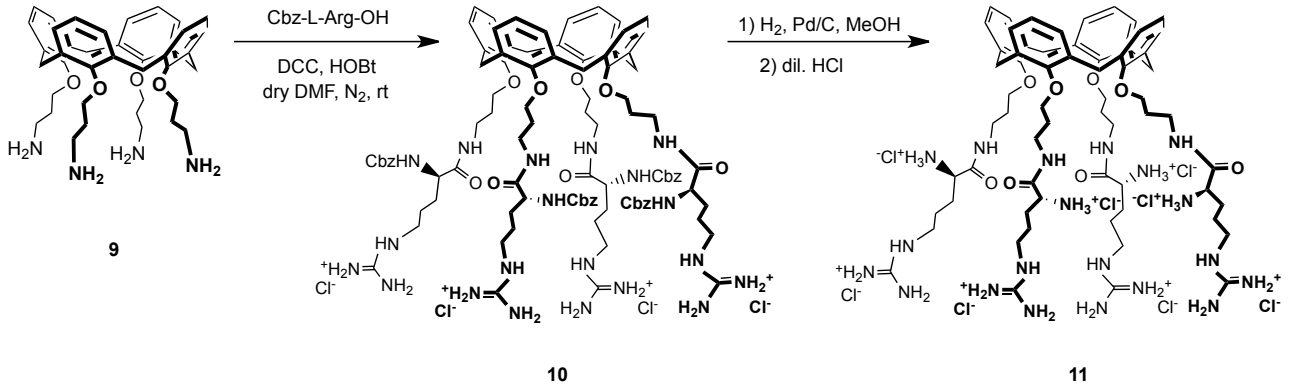

Scheme 3: synthesis of lower rim arginino-calix[4]arene **11**

Deprotection step was then performed under H_2 atmosphere (2 bar) in presence of Pd/C as catalyst. Purification by semipreparative HPLC and freeze-drying from diluted HCl solution (10mM) gave the chloride salt of the desired product **11**.

2.2.2 Aggregation properties in water

The behaviour in water of the three peptido-calixarenes **3**, **5** and **11** and the Gemini derivative **8** was studied through NMR spectroscopy.

The arginino-calixarene **3** was poorly soluble in D_2O. Nevertheless, the ^{1}H-NMR spectrum (**Fig 2.11**) could be registered and evidenced broad signals, even at different temperatures; despite that, signals could be attributed.

The observed signal broadness indicates that this compound tends to self-aggregate as consequence of its amphiphilic character originated by the polar amino acids at the upper rim and the lipophilic hexyl chains at the lower rim.

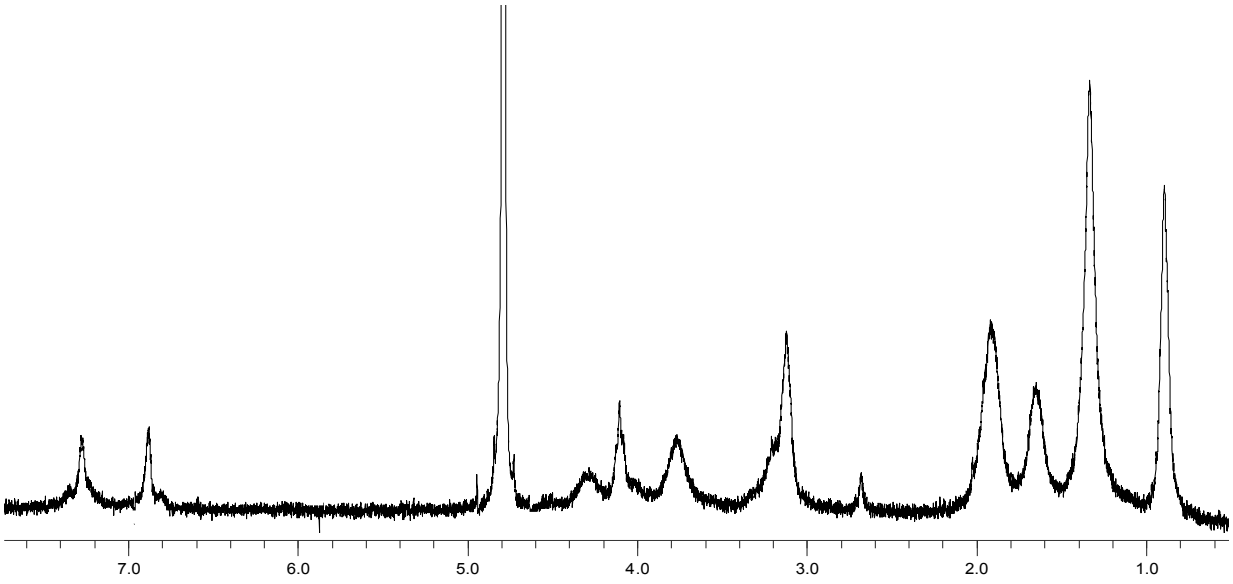

Fig 2.11 ^{1}H NMR spectrum (D_2O, 300 MHz, 298 K) of compound **3**.

On the contrary, its Gemini analogue **8** was well soluble in water and, despite the almost identical functionalization of phenolic units respect **3**, it showed sharp ^{1}H-NMR signals (**Fig 2.12**). The conformational freedom of this acyclic compound probably induces a twisted arrangement of the two units, lacking well defined polar and apolar regions and then amphiphilicity.

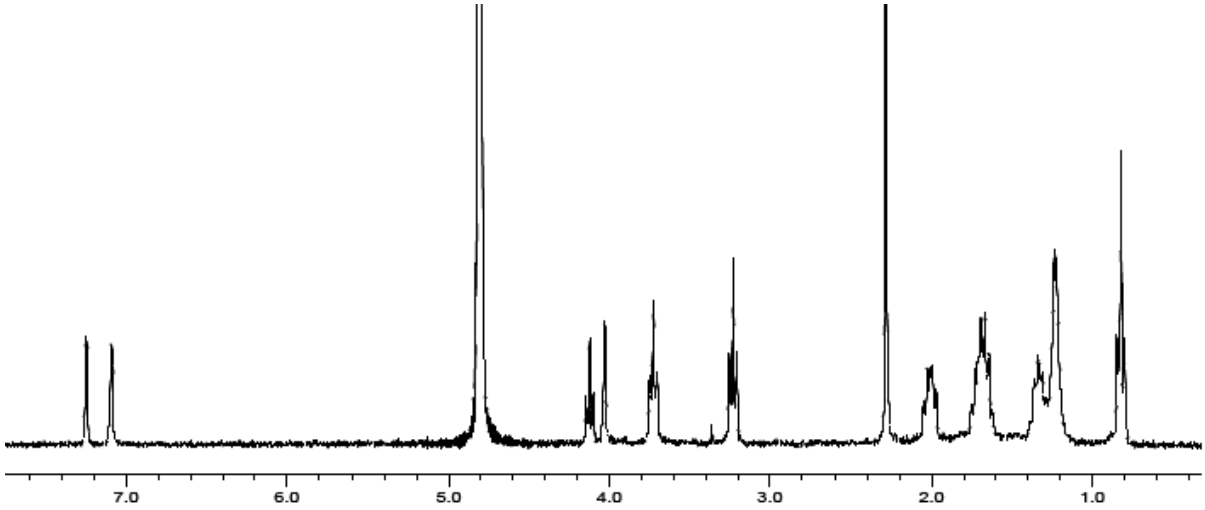

Fig. 2.12 ^{1}H NMR spectrum (D_2O, 400 MHz, 298 K) of compound **8** at 1mM concentration.

Calixarenes **5** and **11** had good water-solubility and gave also sharp spectra. However, a deeper investigation revealed a tendency to aggregation of lysino derivative **5** upon

polarity increase of D_2O solution. The addition of inorganic salts (NaCl and $MgCl_2$, 10 and 2 mM, respectively) (**Fig 2.13 B**), caused the formation of water-soluble aggregates in equilibrium with the monomeric species, as indicated by the simultaneous presence in the spectrum of the protons belonging to the calixarene methylene bridge (two sharp doublets at 4.53 and 3.30 ppm) for the monomer and two broad signals (at 4.33 and 2.21 ppm) for the aggregates. At higher salt concentrations (25 mM NaCl and 5 mM $MgCl_2$) self-association of this amphiphilic calixarene is complete as evidenced by the disappearance of all the sharp signals (**Fig 2.13 C**). No further changes were observed upon increase (**Fig 2.13 D**) of NaCl and $MgCl_2$ salts to 500mM and 100mM, respectively.

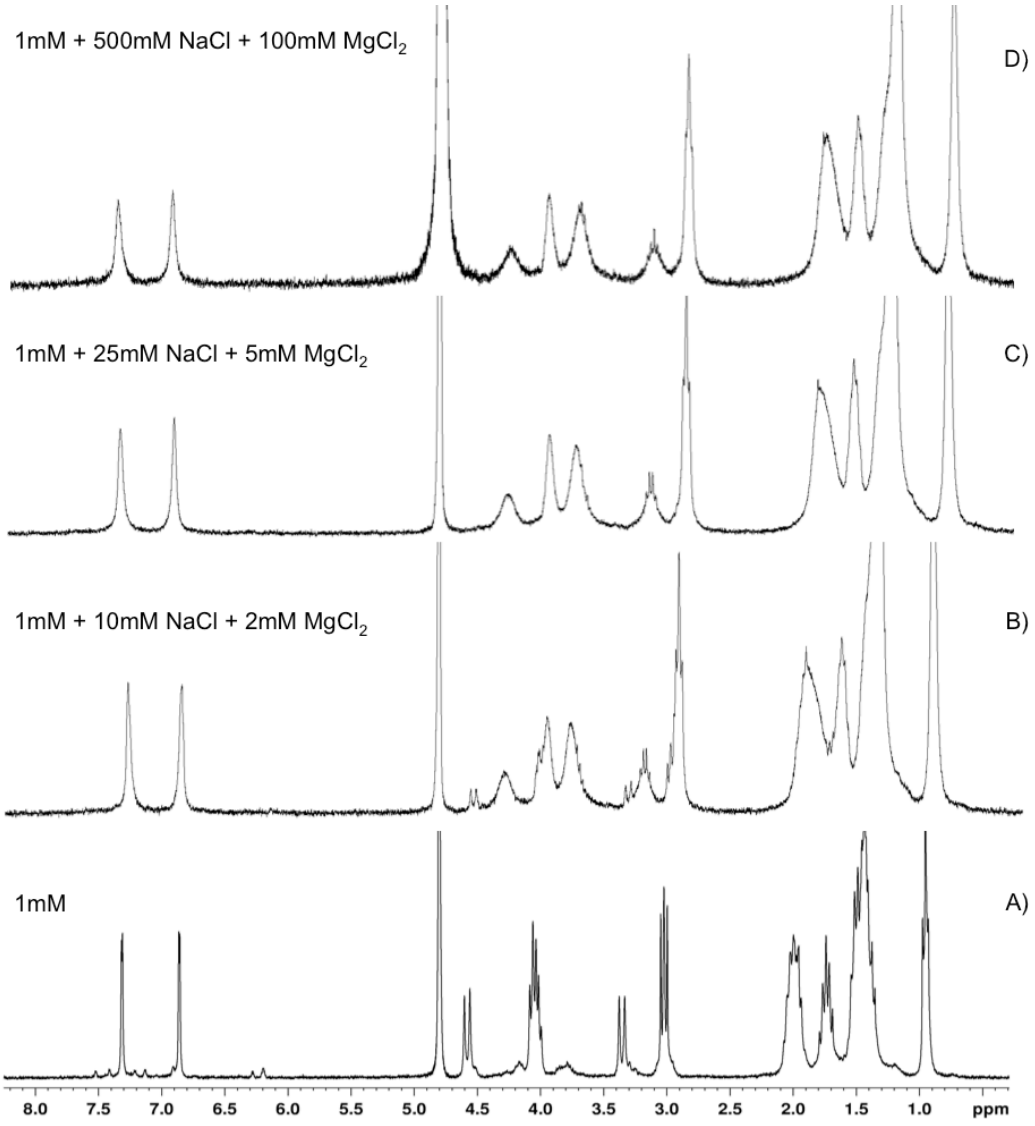

Fig 2.13 ^1H NMR spectra (D_2O, 300 MHz, 298 K) of compound **5,** at concentration 1 mM (A) pure D_2O and (B-D) in presence of increasing concentration of inorganic salts.

Calixarene **11** did not show this aggregation tendency, at least up to the investigated salts' concentrations (**Fig 2.14**). Evidently, the unfunctionalized aromatic rings of the calixarene cavity do not present a sufficient lipophilic character to counterbalance the hydrophilic groups at the lower rim and to allow the formation of aggregates.

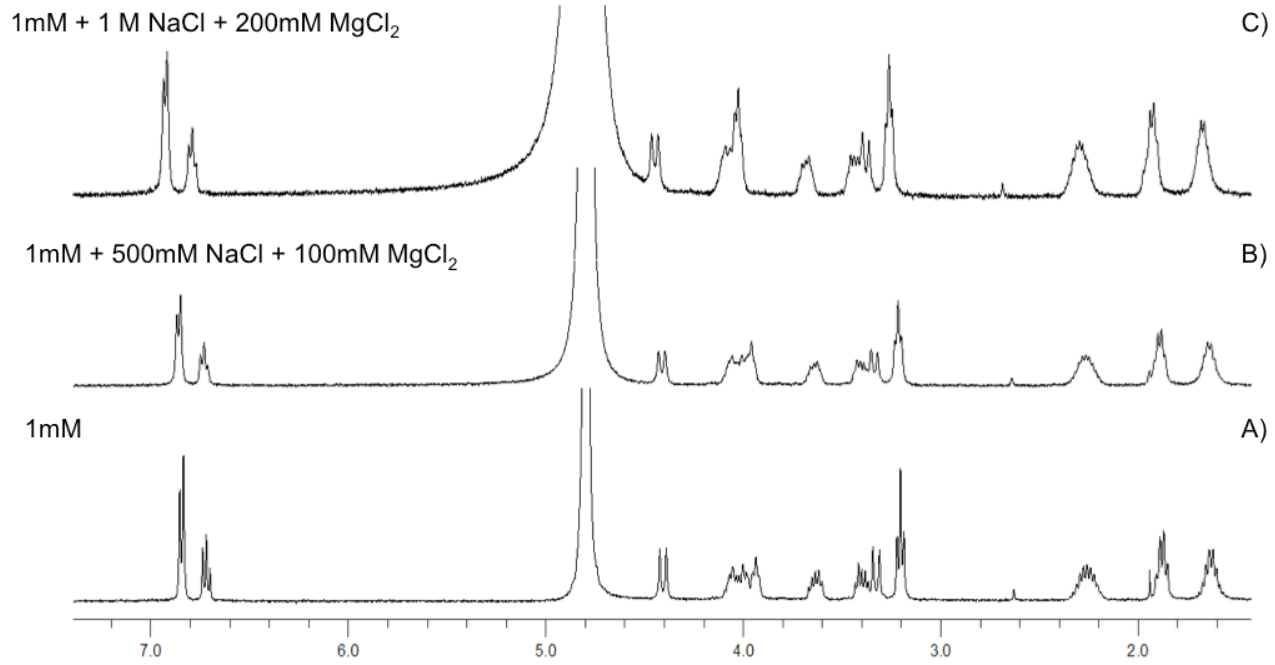

Fig 2.14 ^{1}H NMR spectra (D_2O, 300 MHz, 298 K) of compound **11,** in pure D_2O at concentration 1 μM (A) and in presence of various concentration of inorganic salts (B and C).

2.2.3 DNA binding studies

Before the transfection tests, the obtained compounds were studied with various techniques to verify their binding properties toward DNA. All experiments were performed using the pEGFP-C1 DNA (4731 bp), encoding for the Enhanced Green Fluorescent Protein and subsequently used for cell transfection assays.

The ability of compounds to bind this plasmid was initially assessed through Ethidium Bromide Displacement Assay. Ethidium Bromide (EB) intercalates between the base-pairs of the double helix of the pDNA. When intercalation occurs its fluorescence yield increases. If the ligand binds DNA causing the release of EB in the aqueous environment, the fluorescence decreases. The relative fluorescence at 600 nm (λ max), defined as the ratio between the fluorescence of the complex EB-DNA in presence of ligand and the

fluorescence of the EB-DNA complex alone, usually gives an indication of the interaction strength between the ligand and the DNA. These experiments were conducted titrating a 0.5 nM solution of the DNA-EB complex with a solution of ligand at fixed concentration.
The spectrofluorimetric titration gave only a qualitative indication of the interaction between our ligands and the pDNA. No determination, for example, of association constants was possible because, as it will be shown below in the description of AFM experiments, in our cases the interaction and the EB displacement cannot be simply related to a competitive binding process. Then, also a normal decrease of fluorescence and the change of slope of titration curves could not be exploited to quantitatively determine and compare the complexation strength of different ligands tested. After an initial quenching of fluorescence (**Fig 2.15**), indicating the ability of our compounds to effectively bind to the plasmid, a marked new increase occurred, especially in the case of compounds **3** and **5** (blue and green lines).

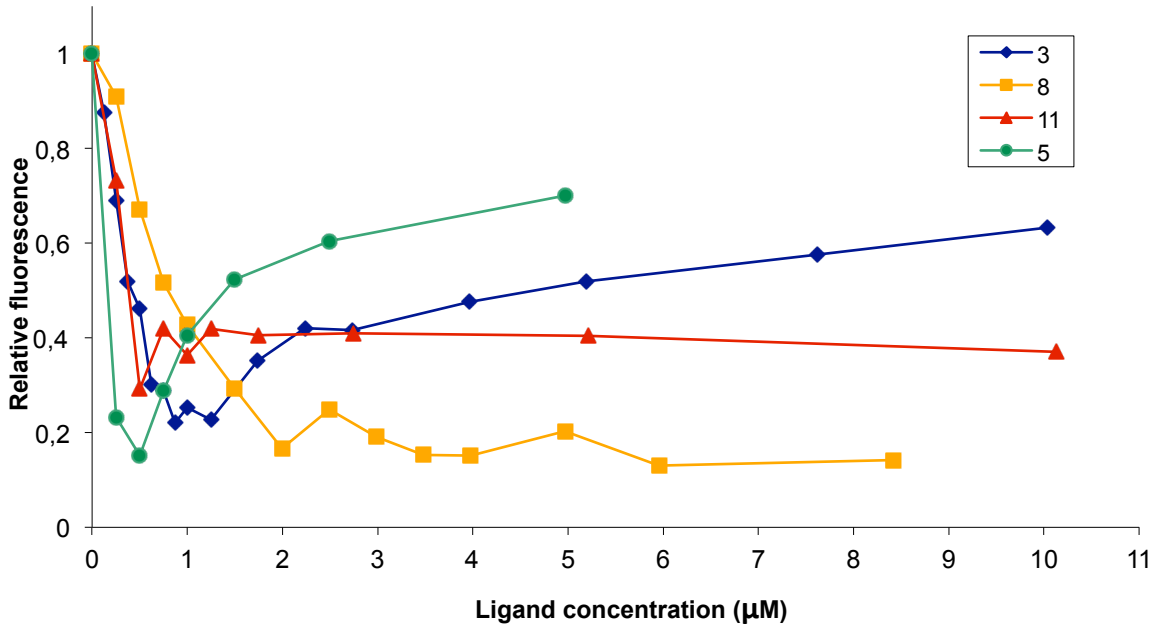

Fig 2.15 Ethidium Bromide Displacement Assays. Relative fluorescence *vs* ligand concentration. Fluorescence studies (excitation at 530 nm, emission at 600 nm) were performed collecting the emission spectra of buffered solutions (4 mM Hepes, 10 mM NaCl) of 50 mM ethidium bromide (relative fluorescence = 0), mixture of 0.5 nM plasmid DNA (pEGFP-C1) and 50 mM ethidium bromide (relative fluorescence = 1) and after addition of increasing amounts of ligand to the DNA/ethidium bromide mixture.

We hypothesized that this change of slope could be due to the formation of aggregated species able to create hydrophobic portions where EB can be placed and turn on its fluorescence again.

Therefore, if we limit our analysis to the decreasing portions of the curves (ligand concentration < 0.5 μM) it would seem that the lysino-calixare **5** is more efficient than the arginine containing compounds **3**, **8** and **11**. Actually, as mentioned above, it is not possible to directly correlate the efficiency of one of these ligands in the EB displacement with its affinity for the plasmid.

A second set of experiments was based on Electrophoresis Mobility Shift Assay (EMSA). In particular we focused our attention on the differences of behaviour of the two calixarenes bearing arginine units (**Fig 2.16**).

These data revealed that is the calixarene **11** the ligand mostly affecting DNA mobility: already at 50μM ("nitrogen"/phosphate group ratio, N/P 2.5), all plasmids remain in the well. Differently, for derivative **3** a higher concentration is needed to get a complete complexation (100μM, N/P 5). In both cases we observed a light staining in the wells due to Ethidium Bromide used to visualize DNA in the gel when all plasmids were retained. This fact seems to be in agreement with the behaviour recorded during the previous fluorimetric titrations. The non macrocyclic ligand **8** was not able to affect the electrophoretic run of plasmid even at 200 μM.

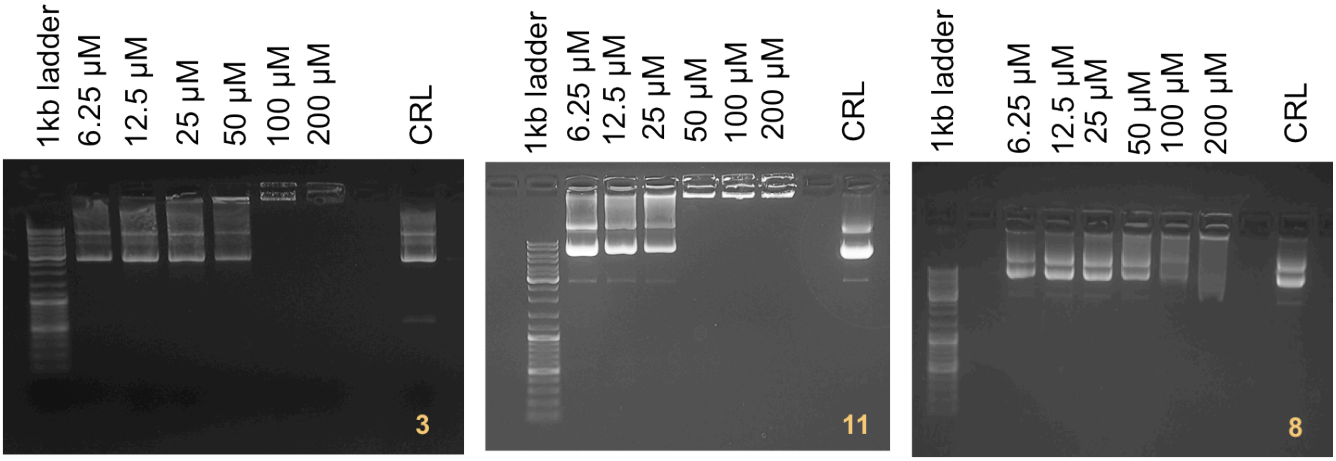

Fig 2.16 EMSA (electrophoretic mobility shift assays) relative to compounds **3**, **11** and **8** at different concentrations, in presence of plasmid DNA (pEGFP-C1)

Very interesting information on the DNA binding properties of our ligands was obtained by atomic force microscopy (AFM), a technique already successfully used to investigate the interaction between different synthetic ligands and DNA. The experiments were performed with the circular plasmid DNA pEGFP-C1 in tapping mode on air. First, the images were

recorded depositing the DNA onto mica in absence of ligand (**Fig 2.17**) and using a buffer rich in Mg^{2+} ions necessary for retaining the filaments on the surface. The filaments appear in the so-called relaxed form. There is some overlapping along the single plasmids but their circular structure can be easily distinguished.

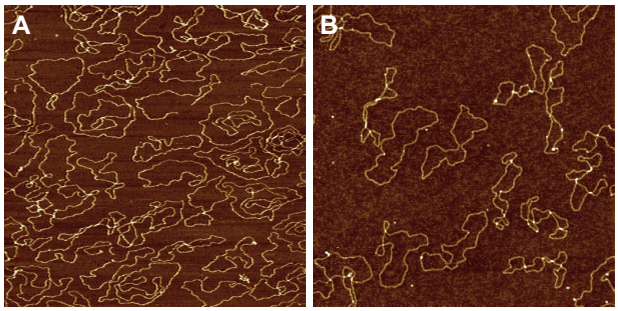

Fig 2.17 AFM images (2x2 μm) of plasmid pEGFP-C1 **A)** at concentration 1 nM; **B)** at concentration 0.5 nM.

Then, images relative to mixtures of the DNA with our ligands were collected after 5 min of incubation. In this way the interaction vector-DNA and how it affects the plasmid folding could be immediately visualized.

The upper rim arginino-calixarene **3** forms highly condensed nanometric aggregates constituted by a single filament already at 2μM (N/P~ 4) (**Fig 2.18**). In this case it was also possible to observe on mica surface very small particles not containing pDNA filaments. This could be ascribed to the macrocycle aggregates, according to the tendency of **3** to self-aggregation previously detected by NMR spectroscopy.

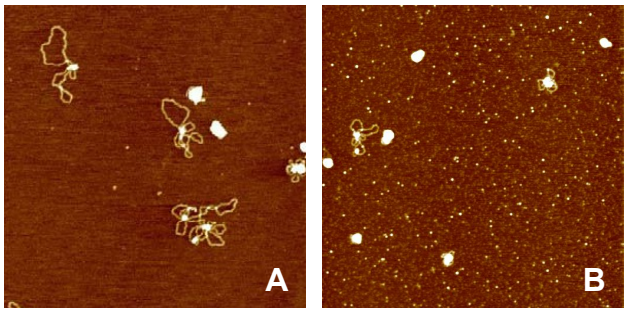

Fig 2.18 AFM images (2×2 μm) showing the effects induced on plasmid DNA (0.5 nM) by ligand **3**. Plasmid incubated with **3** (A) 1 μM and (B) 2 μM.

Higher concentration of **3** prevented the deposition of its pDNA-complexes on the surface, probably because of the complete masking of the plasmid negative charges. The observed

condensates, whose size not exceeding 100 nm, have suitable dimensions to be easily internalized into cell, and in fact **3** already demonstrated its excellent properties in cell transfection. Therefore we widened the investigation on them and estimated their hydrodynamic diameter by Dynamic Light Scattering (DLS), a widely used technique to determine the size distribution profile of small particles in solution. The surface charge of calix-DNA complexes was calculated measuring its Z-potential, by applying an electric field to the sample. We determined these two parameters especially at N/P≥5 used for transfection experiments. The dimensions below 100 nm were confirmed and a positive Z-potential around 50 mV was found (**Fig 2.19**).

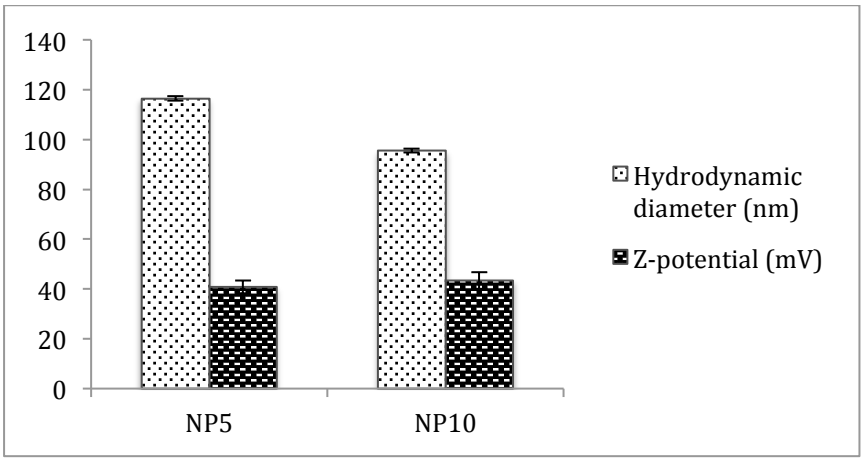

Fig 2.19 Values of hydrodynamic diameter and Z-potential for compound **3** at two different N/P.

The mono-disperse population photographed by AFM and DLS was also by using transmission electron microscopy (TEM).

This technique again confirmed the size and homogeneous distribution of calixarene-pDNA complexes. Moreover, at high magnification, a well-defined internal structure of the aggregate, alternating lamellar arrangements of calixarene (light color) and pDNA (dark color), was observed. Presumably this packing is made possible by the amphiphilic nature of the vector that establishes hydrophobic as well as electrostatic interactions (**Fig 2.20**).

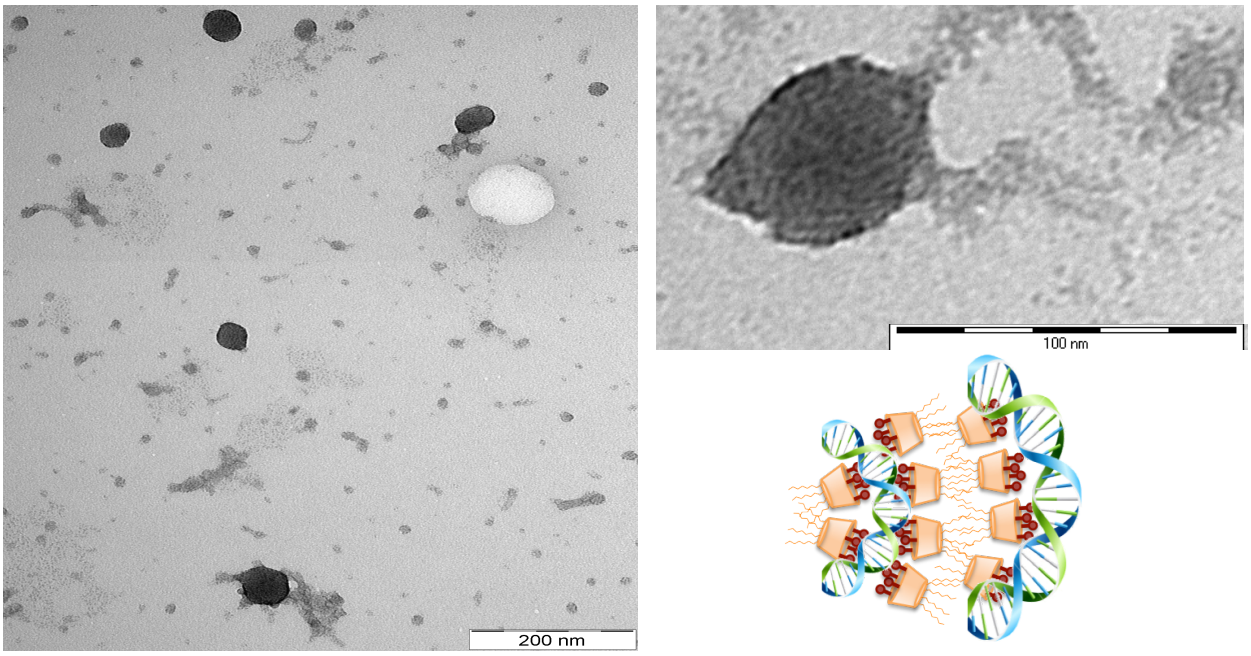

Fig 2.20 TEM image of **3**-pDNA complexes, with amplification of ultrafine structure of aggregates and an schematic representation of a section of the proposed packing.

Performing AFM experiments on Gemini-type derivative **8**, no pDNA condensation was observed (at N/P=4, previously used for **3**) indicating that a higher mobility of the structure negatively affects the properties of the compound as ligand (**Fig 2.21 A**).

Both calixarenes **5** and **11** formed big aggregates constituted by numerous filaments of pDNA, maybe not suitable for transfection (**Fig 2.21 B-D**). However, after the addition of DOPE (dioleoylphosphatidylethanolamine), a helper lipid widely used in transfection experiments, to the solution containing pDNA incubated with the lysino-calixarene **5,** the large aggregates, observed before, were not present on the mica surface. They were replaced by small monofilament condensates with appropriate shape and size for cell uptake (**Fig 2.21 E** and **F**).

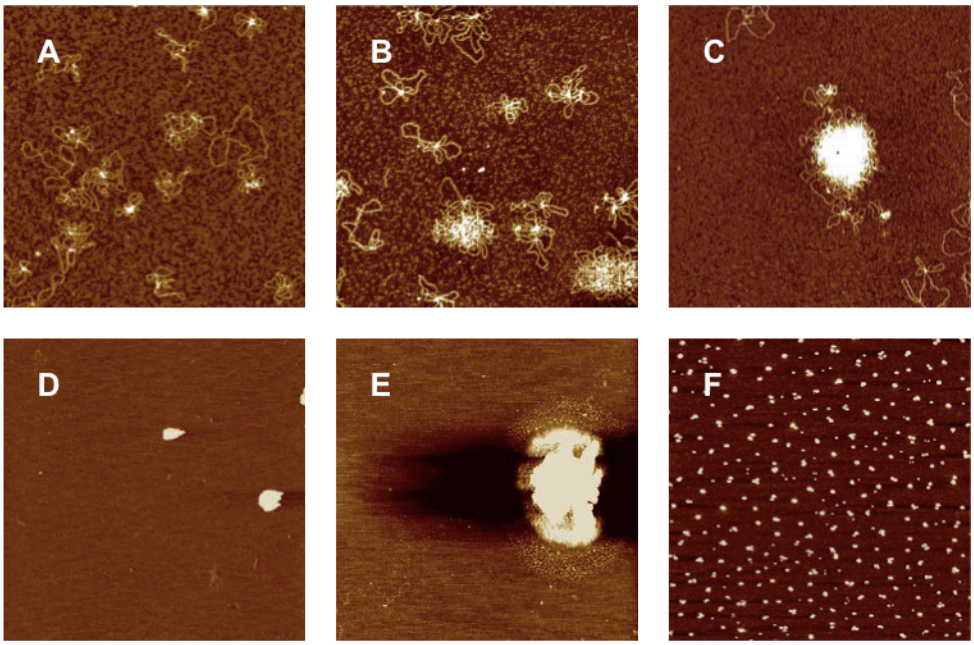

Fig 2.21 AFM images showing the effects induced on plasmid DNA incubated with A) **8** 1 μM (2×2 μm); B) **11** 0.5 μM (2×2 μm); C) **11** 1 μM (2×2 μm); D) **5** 2 μM (5×5 μm); E) **5** 2 μM + DOPE 4 μM after 30 min (2×2 μm); F) **5** 2 μM + DOPE 4 μM after 3 h (2×2 μm).

2.2.4 Transfection properties

On the basis of binding studies, we started to investigate transfection abilities, intrigued by the different behaviours in pDNA condensation possibly affecting the delivery capabilities. These experiments were performed on RD-4 human Rhabdomyosarcoma cells, a human tumor, using plasmid pEGFP-C1 (1nm) encoding for the green fluorescent protein (**Fig 2.22**). The production of the latter one in cells is detectable by fluorescence microscopy and allows us to easily quantify transfection efficiency of our vectors. RD-4 cell line was chosen because of its medical relevance and difficulty to be transfected by traditional protocols.

The results we obtained in the treatment of these cells were in very good agreement with the phenomena photographed by AFM.

The lower rim arginino-calixarene **11** resulted a very poor vector; only in presence of adjuvant DOPE was able to transfect 5% of cells. It was also a worse transfecting agent than the corresponding lower rim guanidino-calix[4]arene **I** able to give 40% of transfected cells in presence of DOPE). [26b,c]

On the contrary, the activity shown by the upper rim arginino-calix[4]arene **3** was impressive: Used alone (10μM, N/P=8.4) it resulted able to transfect 80% of treated cells. Rather surprisingly, this percentage decreased to 46% when DOPE was added. However, in both cases the transfection efficiency was higher than those achieved by the commercially available lipofectamine LTX^{TM} (35%) and PEI (40%), used as references, being well-established transfectants in common protocols.

Experiments on its Gemini-analogue **8** confirmed the previously collected data. It showed very limited binding and condensation abilities and, consequently, did not give efficient cell transfection showing less than 10% of transfection with DOPE.

Particularly striking is the comparison with the upper rim lysino-calixarene **5**. Practically, no transfection occurred when this ligand was used alone and this behaviour is consistent with the data collected by AFM. It is also quite interesting to note the dramatic difference between the efficiency of the cluster **3** based on arginine and that of cluster **5** based on lysine. In this arrangement the guanidinylated amino acid is definitely superior to the ammonium-based one. Again in agreement with the AFM observations, when DOPE was used in the formulation for transfection, the efficiency of **5** increased up to 45%. It is important to underline that DOPE alone does not show any transfection ability.

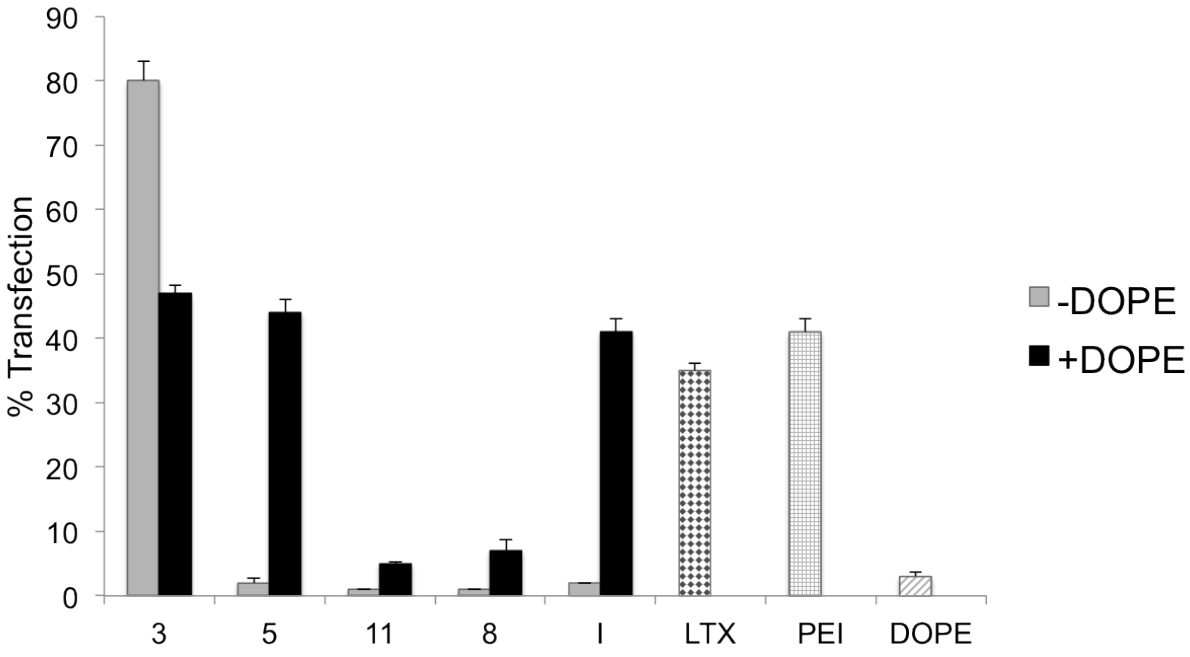

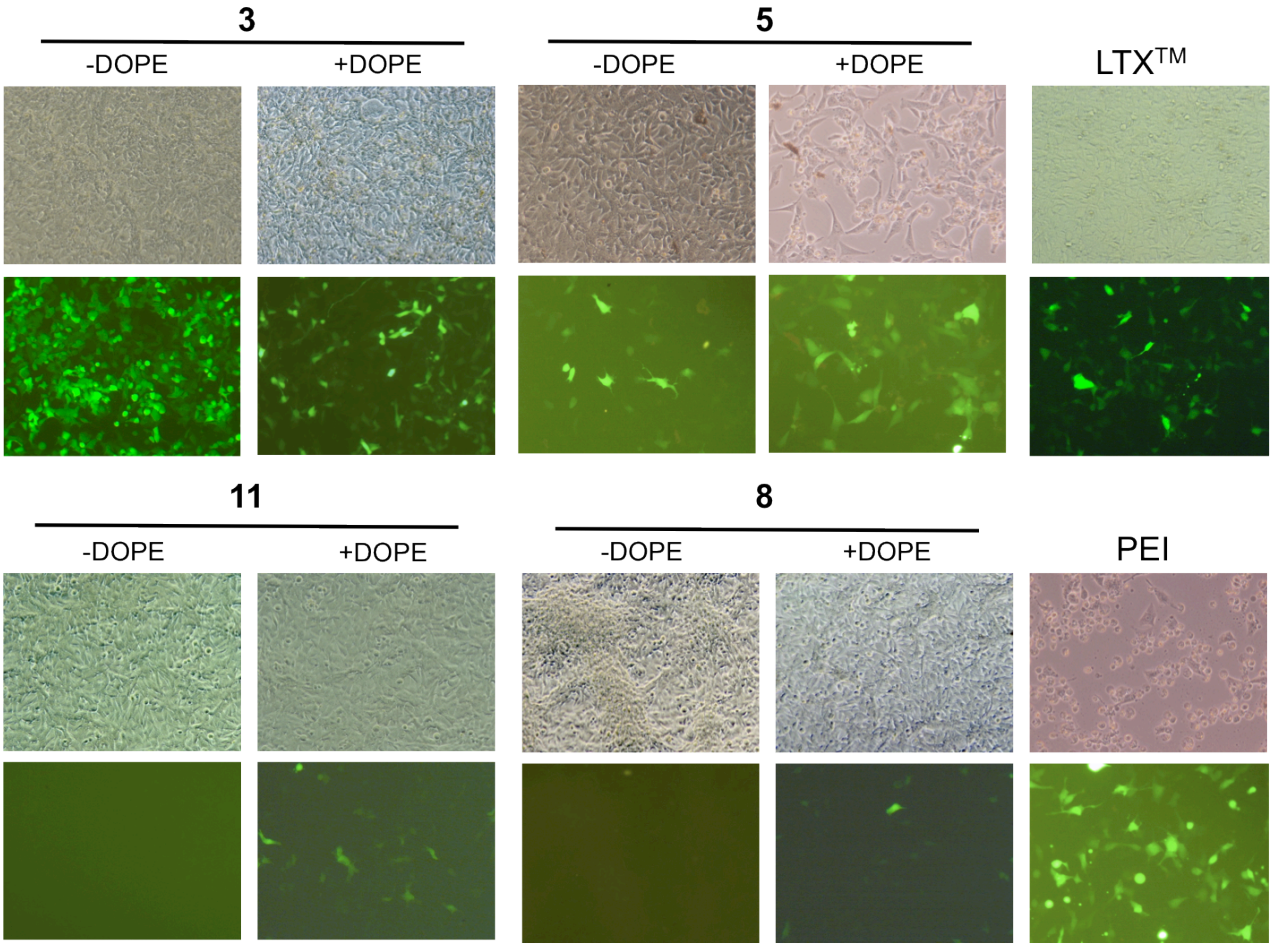

Fig 2.22 Transfection experiments performed with 1nM pEGFP-C1 plasmid, synthesized compounds, alone (-DOPE) and in presence of DOPE (+DOPE: 1/2 molar ratio, 10/20 μM), and lipofectamine LTX, PEI and DOPE to RD-4 cells. Upper image: in vitro transfection efficiency as percentage of transfected cells upon treatment with ligands **3**, **5**, **8** and **11**, alone and in presence of DOPE (1/2 molar ratio, 10/20 μM), the lower rim guanidino-calix[4]arene **I**, LTX, PEI and DOPE. Lower images: phase contrast images and fluorescence microscopy images of the transfected cells.

On the whole the presence of the helper lipid, apart the case of ligand **11** and **8** for which no significant changes are obtained, seems to level the efficiency (around 45%) of our vectors, including in the comparison the guanidino-calixarene **I**. For the very active arginino-derivative **3**, in fact, the efficiency is reduced to a value to which that one of **5** and **I** is, on the contrary, pushed up.

The superiority of **3** respect to other ariginino-derivatives (**8** and **11**) and LTX was also confirmed by transfection experiments based on luciferase report assay (**Fig 2.23**).

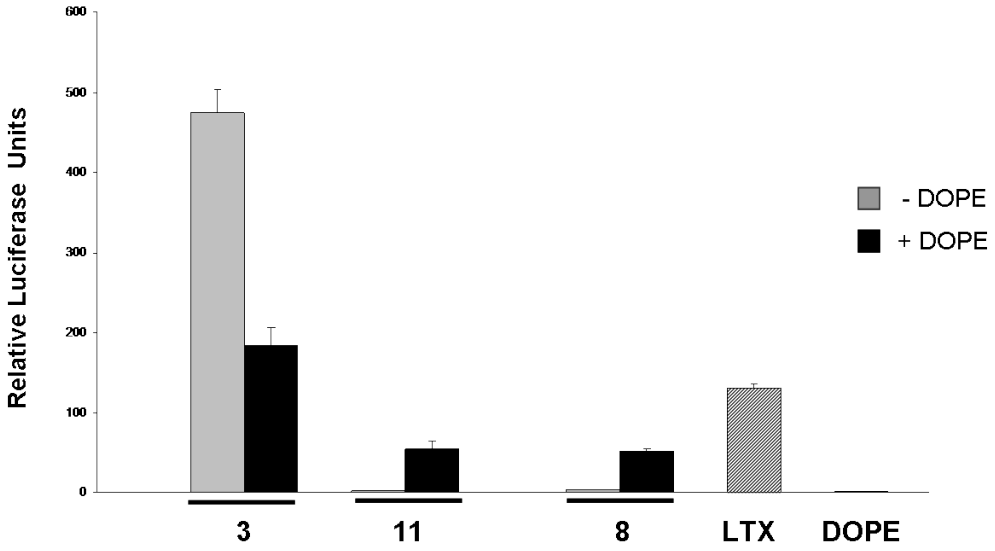

Fig 2.23 In vitro transfection efficiency upon treatment with ligands **3**, **8** and **11**, alone (-DOPE) and in presence of DOPE (+DOPE: 1/2 molar ratio, 10/20 μM), LTX and DOPE as determined by luciferase report assay.

Encouraged by these good results, we decided to test our promising carrier **3** in presence of 10% serum in the transfecting solutions, to reach conditions closer to the physiological ones. Green fluorescence protein expression in RD-4 cells showed a decrease of only 20% respect to the previous conditions, confirming the high efficiency of compound **3** and the potential of this compound as non viral vector (**Fig 2.24**).

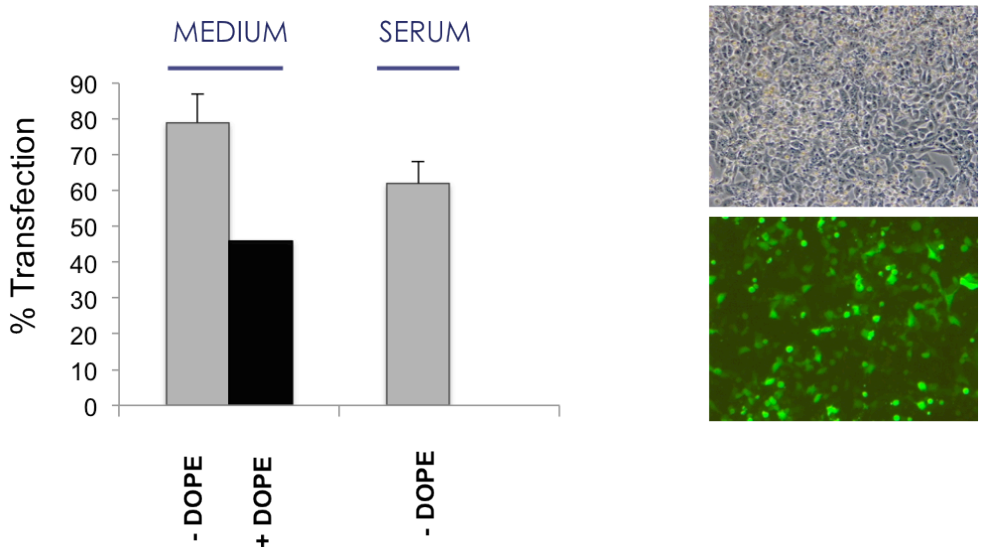

Fig 2.24 Transfection experiments performed with 1nM pEGFP-C1 plasmid and arginino-calixarene **3**, in presence of 10% of serum in transfection mixture, on RD-4 cells. Left image: in serum transfection efficiency as percentage of transfected cells Right images: phase contrast images and fluorescence microscopy images of the transfected cells.

Quite rewarding was also the finding that the most active compounds **3** had low cytotoxicity, showing 77% of cell viability in MTT assays at 48h in transfection conditions on RD-4 cells (**Fig 2.25**). Considering that the LTX's percentage of cell viability is around 85%, the value found for **3** is really encouraging. The cell viability slightly decreases (70%) in presence of DOPE. This is rather surprising since this adjuvant is also in general used to limit toxicity. For the lysino-cluster **5** the % of cell viability in presence of DOPE, necessary in this case to have significant transfection activity, was 62%, lower than in absence but however still acceptable.

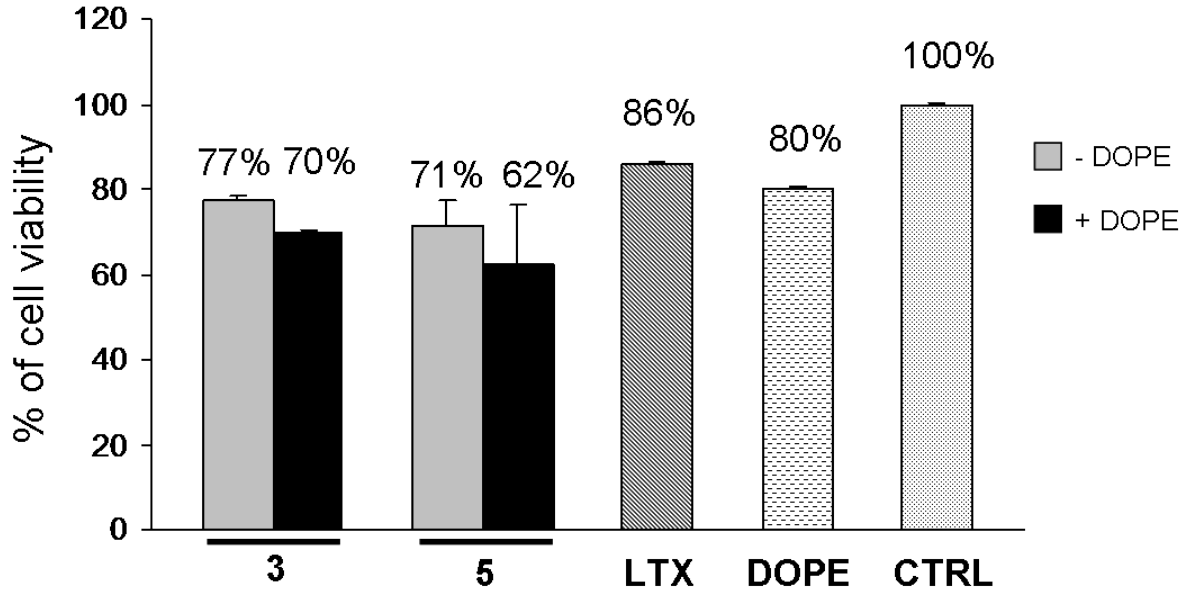

Fig 2.25 Percentage of cell viability of ligand **3** and **5** on RD-4 cells at 48 h from the treatment in MTT assays, in transfection conditions.

Since it is well known in the development of non viral vectors that transfection efficiency may strongly depend on the type of cells used, the peptido-calixarenes **3** and **5** were also tested in a various cell line settings using again LTX^{TM} and PEI as references (**Fig 2.26**).

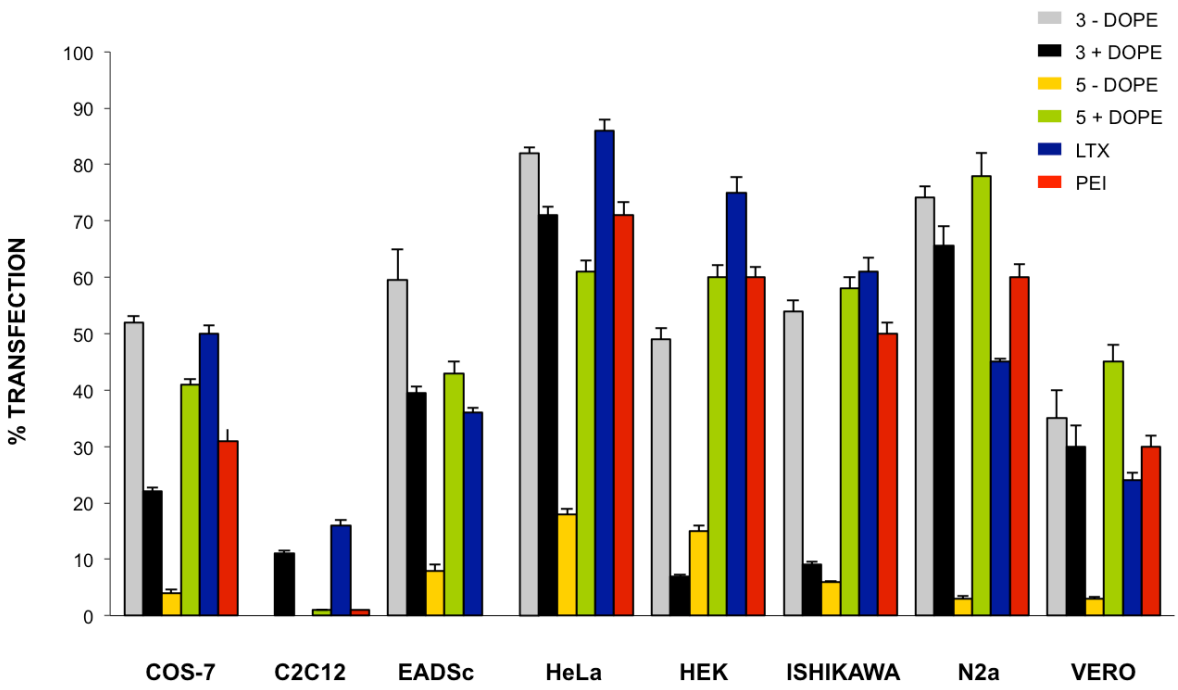

Fig 2.26 In vitro transfection efficiency as percentage of transfected cells upon treatment with calixarenes **3** and **5**, alone (-DOPE) and in presence of DOPE (+DOPE: 1/2 molar ratio, 10/20 μM), LTX and PEI, as references, on different cell lines.

Apart the C2C12 line to which both ligands resulted inactive and LTX and PEI also have a very poor efficiency, in all other cases the superiority of the arginino-calixarene **3** over the lysino analogue **5** appeared unequivocal without the use of DOPE (-DOPE). While for the latter one, a maximum of 18% of transfected cells was observed in the case of Hela, with **5** more than 80% of transfection was obtained in the treatment of this cell line, more than 70% with N2a, 60% with EADSCs, more than 50% with COS-7 and 40% with Vero cells. Moreover, excluding the cases of HEK cells where LTX showed a significantly larger efficiency (75% *vs* ca 50%) and the above mentioned C2C12 cells, arginino-calixarene **5** always resulted characterized by a transfection activity higher or at least comparable with those of both references LTX and PEI or one of them. With EADSCs cell line, for instance, PEI was completely inefficient while 60% of transfection was obtained upon treatment with **5** that also almost doubled LTX (36%).

As in the experiments with RD-4 cells, the presence of DOPE in general decreased the efficiency of **3**, in some cases also drastically (COS-7, HEK, ISHIKAWA lines), even if determined a small activity with C2C12 not transfected at all in absence of adjuvant. On the contrary the helper boosted the activity of the lysino-calixarene **5** that reached (EADSc and HeLa) or even surpassed (COS-7, HEK, ISHIKAWA, N2a and Vero cells) the

transfection efficiency of arginino-cluster **3** evidently partially inhibited in the presence of DOPE respect to its use alone.

With **3**, in the case of N2a cells we observed a significant increase of the transfected cells, from 50% at 24 h to more than 70% at 48 h from the treatment while, on the contrary, in the presence of DOPE the percentage was stable at 65%. This seems to suggest that the helper, at least in the transfection of some cell lines, mainly speeds up the gene delivery process.

2.3 Conclusions

In conclusion, the clustering of only four amino acid units on a rigid macrocyclic scaffold such as a cone calix[4]arene displaying two spatially well-defined regions, one apolar at the lower rim and one polar at the upper, gives rise to new potent non viral vectors for cell transfection. In the particular case of derivatives functionalized at the upper rim, the one to one ratio between amino acid units and lipophilic tails is enough to reach remarkable results, especially in the case of the upper rim arginino-calixarene **3** This indicates that the circular array provided in this ensemble particularly boosts the cell penetrating properties that basic amino acids usually show in linear oligomeric sequences (at least 8 arginine units per lipophilic chain). Moreover, this novel arginine arrangement present in **3** also makes additional primary amino groups available, which might favor the protection of the vector-DNA complex from the lisosomial degradation and facilitate the release of DNA from the endosomes inside the cytosol, through the proton sponge effect and thus increasing the transfection efficiency of the vector.

All these features make vector **3** the potential progenitor of a new class of synthetic cationic lipids which could constitute a valuable alternative to commercially available formulations in transfection protocols and suggest an unprecedented approach for the presentation of arginines in designing novel efficient cell penetrating agents.

Interestingly, despite the known use of polylysines in gene delivery, the arrangement of this amino acid failed in providing for calixarene **5** transfection activity when used alone. On the other hand the presence of DOPE as adjuvant furnished to this compound the ability to transfect cells with efficiency, comparable with or higher than LTX and PEI.

Comparison of the DNA condensation and cell transfection efficiency of the most active compound **3** with its open chain analogue **8**, having a very similar lipophilic/hydrophilic ratio, suggests a possible positive role of the macrocyclic scaffold on gene delivery to cell.

Some hypotheses can be put forward to explain in particular the worse performance of the lower rim arginino-calix[4]arene **11** as non-viral vector compared to its upper rim analogue. The failure of **11** as gene delivery system can be ascribed to the absence of a significant lipophilic region sufficient to counterbalance the polarity of the substituents at the lower rim. Moreover, the shape of this ligand and the volume occupied by the polar heads with respect to the lipophilic portion constituted only by the aromatic nuclei is apparently not suitable to induce aggregation phenomena able to support a transfection activity.

2.4 Experimental section

General Information. All moisture sensitive reactions were carried out under nitrogen atmosphere, using previously oven-dried glassware. All dry solvents were prepared according to standard procedures, distilled before use and stored over 3 or 4 Å molecular sieves. Most of the solvents and reagents were obtained from commercial sources and used without further purification. Analytical TLC were performed using prepared plates of silica gel (Merck 60 F-254 on aluminum) and then, according to the functional groups present on the molecules, revealed with UV light or using staining reagents: $FeCl_3$ (1% in H_2O/CH_3OH 1:1), ninhydrin (5% in EtOH), basic solution of $KMnO_4$ (0.75% in H_2O). Reverse phase TLC were performed by using silica gel 60 RP-18 F-254 on aluminum sheets. Merck silica gel 60 (70-230 mesh) was used for flash chromatography and for preparative TLC plates. ^1H NMR and ^{13}C-NMR spectra were recorded on Bruker AV300, Bruker AV400 and Varian Inova 600 spectrometers (observation of ^1H nucleus at 300 MHz, 400 MHz and 600 MHz respectively, and of ^{13}C nucleus at 75 MHz, 100 MHz and 150 MHz respectively). All chemical shifts are reported in part per million (ppm) using the residual peak of the deuterated solvent, which values are referred to tetramethylsilane (TMS, $\delta_{TMS} = 0$), as internal standard. All ^{13}C NMR spectra were performed with proton decoupling. For ^1H NMR spectra recorded in D_2O at values higher than the room temperature, the correction of chemical shifts was performed using the expression δ = 5.060−0.0122 × T (°C) + (2.11 × 10−5) × T2 (°C) to determine the resonance frequency of water protons (Gottlieb, H. E., Kotlyar, V., and Nudelman, A. *J. Org. Chem.* **1997**, *62*, 7512−7515). Electrospray ionization (ESI) mass analyses were performed with a Waters spectrometer. HRESI-MS spectra were recorded on a LTQ Orbitrap XL instrument in positive mode with MeOH as solvent. Melting points were determined on an Electrothermal

apparatus in closed capillaries.

Nomenclature of calix[4]arene compounds. In this thesis the simplified nomenclature proposed by Gutsche is used to name the calix[4]arene compounds. The positions on the macrocycle are numbered as indicated in the following figure. The hydroxyl substituent defines the ipso position: subsequently the ortho, meta and para positions on the aromatic rings are identified without ambiguity.

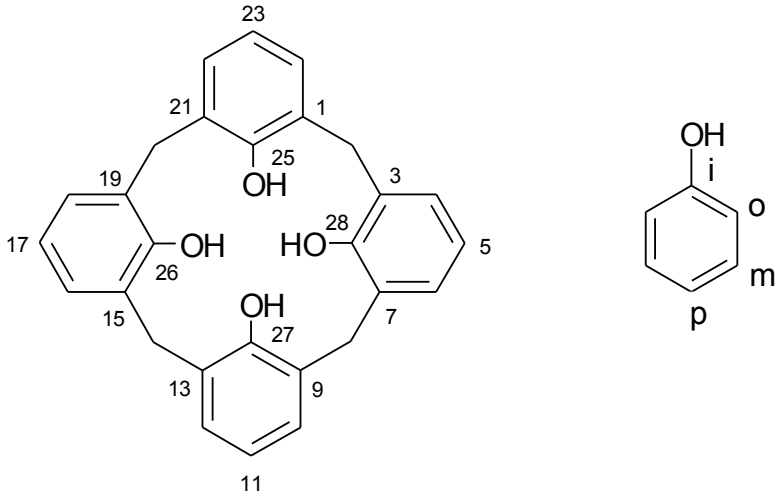

Synthesis of 5,11,17,23-Tetramino-25,26,27,28-tetrakis(*n*-hexyloxy)calix[4]arene (1)

It was synthesized according to a literature procedure. [26a]

Synthesis of 25,26,27,28-Tetrakis(3-aminopropoxy)calix[4]arene (9)

It was synthesized according to a literature procedure. [30]

Synthesis of Boc-L-Lysine(Boc)-OH

It was synthesized according to a literature procedure.[31]

Synthesis of Bis[(2-hexyloxy-3-methyl-5-nitro)phenyl]methane

To a solution of bis[(2-hexyloxy-3-methyl-5-*tert*-butyl)phenyl]methane **6** (1.05 g, 2.065 mmol) in trifluoroacetic acid (4.70 mL, 61.17 mmol), $NaNO_3$ (3.45 g, 40.70 mmol) was added. After one night the reaction was stopped with addition of water (100 mL) and extracted with CH_2Cl_2 (2×50 mL). The separated organic layer was washed with water (75

mL), dried over anhydrous Na_2SO_4 and concentrated under reduced pressure. The residue was purified by flash column chromatography on silica gel (eluent: hexane/ethyl acetate= 98:2) to obtain the pure product as light yellow oil in 60% yield.

^{1}H NMR (300 MHz, $CDCl_3$) δ 7.99 (d, *J* = 2.8 Hz, 2H, Ar*H*), 7.77 (d, *J* = 2.8 Hz, 2H, Ar*H*), 4.10 (s, 2H, ArCH_2Ar), 3.81 (t, *J* = 6.6 Hz, 4H, OCH_2), 2.38 (s, 6H, ArCH_3), 1.79 (quint, *J* = 6.6 Hz, 4H, OCH_2CH_2), 1.55-1.25 (m, 12H, $O(CH_2)_2CH_2CH_2CH_2$), 0.89 (t, *J* = 6.7 Hz, 6H, CH_2CH_3).

^{13}C NMR (75 MHz, $CDCl_3$) δ 161.4, 143.5, 134.1, 132.8, 125.3 and 123.6 (*C* Ar), 73.4 (OCH_2), 31.6 ($OCH_2CH_2CH_2$), 30.3 (ArCH_2Ar), 30.2 (OCH_2CH_2), 25.6 ($CH_2CH_2CH_3$), 22.5 (CH_2CH_3), 16.8 (ArCH_3), 13.9 (CH_2CH_3).

ESI-MS (m/z): $[M + Na]^+$ calcd for $C_{27}H_{38}N_2O_6$ 509.3, found 509.4.

Synthesis of Bis[(2-hexyloxy-3-methyl-5-amino)phenyl]methane (7).

To a solution of bis[(2-hexyloxy-3-methyl-5-nitro)phenyl]methane (0.22 g, 0.45 mmol) and hydrazine monohydrate (0.22 mL, 4.52 mmol) in EtOH (14 mL), a catalytic amount of Pd/C was added and the reaction mixture was stirred and refluxed overnight. The pure amine **7** was obtained after evaporation of the solvent under reduced pressure as a light yellow oil in 78% yield.

^{1}H NMR (300 MHz, $CDCl_3$) δ 6.34 (d, *J* = 2.7 Hz, 2H, Ar*H*), 6.17 (d, *J* = 2.7 Hz, 2H, Ar*H*), 3.90 (s, 2H, ArCH_2Ar), 3.69 (t, *J* = 6.9 Hz, 4H, OCH_2), 3.30 (bs, 4H, NH_2), 2.23 (s, 6H, ArCH_3), 1.76 (quint, *J* = 6.9 Hz, 4H, OCH_2CH_2), 1.46 (bquint, *J* = 5.4 Hz, 4H, $O(CH_2)_2CH_2$), 1.42-1.28 (m, 8H, $O(CH_2)_3CH_2CH_2$), 0.91 (t, *J* = 6.9 Hz, 6H, CH_2CH_3).

^{13}C NMR (75 MHz, $CDCl_3$) δ 148.5, 142.0, 134.6, 131.4, 115.7, 115.0 (*C* Ar), 73.2 (OCH_2), 31.8 ($OCH_2CH_2CH_2$), 30.3 (OCH_2CH_2), 29.0(ArCH_2Ar), 25.8 ($CH_2CH_2CH_3$), 22.6 (CH_2CH_3), 16.4 (ArCH_3), 14.0 (CH_2CH_3).

ESI-MS (m/z): $[M + H]^+$ calcd for $C_{27}H_{42}N_2O_2$ 427.3, found 427.5, $[M + Na]^+$ calcd 449.3, found 449.5.

Synthesis of 5,11,17,23-Tetrakis[(Boc-L-Arg(Pbf))amino]-25,26,27,28-tetrakis(*n*-hexyloxy)calix[4]arene (2)

To a solution of Boc-L-Arg(Pbf)-OH (0.58 g, 1.09 mmol) and DMAP (0.27 mg, 2.19 mmol) in dry CH_2Cl_2 (15 mL), HOBt (0.17 g, 1.24 mmol) and EDC [(1-Ethyl-3-(3-dimethyllaminopropyl)carbodiimide hydrochloride] (0.21 g, 1.09 mmol) were added and the

mixture stirred for 15 min. Then, aminocalixarene **1** (0.15 g, 0.18 mmol) dissolved in CH_2Cl_2 was added. The reaction proceeded at room temperature for 24 h. The reaction was quenched by addition of water and the organic layer washed with water (2×25 mL) and saturated $NaHCO_3$ aqueous solution (2×25 mL). The organic solvent was removed at reduced pressure giving a crude material that was purified by flash column chromatography (gradient from CH_2Cl_2 to CH_2Cl_2/MeOH 95:5). The pure product was isolated as a white solid in 40% yield. The product shows the same physical and spectroscopic properties reported in Ref. 28

Synthesis of 5,11,17,23-Tetrakis[(Boc-L-Lys(Boc)amino]-25,26,27,28-tetrakis(*n*-hexyloxy)calix[4]arene (4)

To a stirring solution of Boc-L-Lys(Boc)-OH (0.14 g, 0.36 mmol) and DIPEA (0.06 mL) in dry CH_2Cl_2 (5 mL), HBTU (0.16 g, 0.42 mmol) and aminocalixarene **1** (0.05 g, 0.06 mmol) were added. The mixture proceeded at room temperature for 24 h. Then the reaction was quenched by adding water (6 mL), the organic layer separated and washed with brine (6 mL), and dried over anhydrous $MgSO_4$. After filtration, the solvent was removed at reduced pressure and the pure product was isolated by flash column chromatography (gradient from CH_2Cl_2 to CH_2Cl_2/MeOH 95:5) as white solid in 69% yield.

Mp: 182.0-185.4 °C. ^{1}H NMR (300 MHz, $CDCl_3/CD_3OD$ 19/1) δ 7.10 (bs, 4H, Ar*H*), 6.32 (bs, 4H, Ar*H*), 4.34 (d, *J* = 13.2 Hz, 4H, ArCH_{ax}Ar), 4.05 (bs, 4H, COC*H*NHBoc), 3.87-3.60 (m, 8H, OCH_2), 3.12-2.87 (m, 12H, ArCH_{eq}Ar and CH_2NHBoc), 1.79 (bs, 16H, OCH_2CH_2 and $COCHCH_2$), 1.59 (bs, 8H, $CH_2CH_2NH_3^+$), 1.80-1.20 (m, 104H, $(CH_3)_{3\ Boc}$, $COCHCH_2CH_2$ and $O(CH_2)_2CH_2CH_2CH_2$), 0.85 (bs, 12H, CH_2CH_3).

^{13}C NMR (150 MHz, $CDCl_3/CD_3OD$ 19/1) δ 170.9, 156.3 and 156.0 (*C*=O), 153.5, 135.1, 131.3, 121.2 and 119.8 (*C* Ar), 79.9 and 79.1 ($C(CH_3)_3$), 75.1 (OCH_2), 54.7 (CO*C*HNHBoc), 39.9 (CH_2NHBoc), 32.0 ($OCH_2CH_2CH_2$), 31.1 (OCH_2CH_2), 30.0 ($ArCH_2Ar$), 29.4 ($COCHCH_2$), 29.0 ($CH_2CH_2NH_3^+$), 28.5 and 28.3 ($C(CH_3)_3$), 25.9 ($CH_2CH_2CH_3$), 22.7 ($COCHCH_2CH_2$), 22.5 (CH_2CH_3), 14.1 (CH_2CH_3).

ESI-MS (m/z): $[M + 2Na]^{++}$ calcd. for $C_{116}H_{188}N_{12}O_{24}$ 1089.7, found 1090.2.

Synthesis of 25,26,27,28-Tetrakis{3-[(N_α-Cbz-L-Arg)amino]propoxy}calix[4]arene, tetra-hydrochloride (10)

To a stirring solution of N_α-Cbz-L-Arg-OH (0.79 g, 2.58 mmol) in dry DMF (10 mL), HOBt (0.4 g, 2.92 mmol) and DCC (0.54 g, 2.58 mmol) were added. After 15 min, a solution of calix[4]arene **9** (0.28 g, 0.43 mmol) in dry DMF (10 mL) was added dropwise to the mixture. After 5 days 1.2 eq. of HOBt and 1 eq. of DCC were added and the reaction stirred for 2 days longer. The reaction was quenched by filtration of DCU using a Gooch 5 funnel and by evaporation of solvent under reduced pressure. The crude was further purified by a trituration in diethyl ether (5 mL), it was dissolved in MeOH (5 mL) and eluted through anionic exchange sorbent SAX (ammonium form, Cl^-) to obtain **10** as a white solid in 76% yield.

Mp: 107-110 °C. ^{1}H NMR (300 MHz, CD_3OD) δ 7.42-7.20 (m, 20H, ArH_{Cbz}), 6.70-6.42 (m, 12H, Ar*H*), 5.15-4.93 (m, 8H, C$H_{2\ Cbz}$), 4.37 (d, *J*=13.1 Hz, 4H, ArCH_{ax}Ar), 4.26-4.09 (m, 4H, COC*H*NH), 4.00-3.76 (m, 8H, OCH_2), 3.50-3.31 (m, 4H, OCH_2CH_2CH), 3.25-3.03 (m, 16H, ArCH_{eq}Ar, CH_2NH and OCH_2CH_2CH), 2.28-2.00 (m, 8H, OCH_2CH_2), 2.00-1.49 (m, 16H, $COCHCH_2CH_2$).

^{13}C NMR (100 MHz, CD_3OD) δ 174.8 and 174.4 (*C*=O), 158.9 and 158.8 (*C*=N), 158.7 and 158.6 (*C*=O), 157.7 (*C* Ar $_{calix}$), 138.3 and 138.2 (*C* Ar $_{Cbz}$), 136.4 (*C* Ar $_{calix}$), 129.7, 129.3and 129.2 (*C* Ar $_{Cbz}$) 129.0 and 123.5 (*C* Ar $_{calix}$), 74.1 (OCH_2), 68.0 and 67.9 ($CH_{2\ Cbz}$), 56.5 and 55.2 (CO*C*HNHCbz), 42.2 and 42.1 (CH_2NH), 38.3 (N=CNHCH_2), 32.1 ($COCHCH_2$), 31.5 (OCH_2CH_2), 29.0 (ArCH_2Ar), 26.9 and 26.7 ($COCHCH_2CH_2$).

ESI-MS (m/z): $[M + 3H - 4HCl]^{3+}$ calcd for $C_{96}H_{128}Cl_4N_{20}O_{16}$ 605.3, found 605.5.

Bis{[(5-Boc-L-Arg(Pbf)-amino]-2-hexyloxy-3-methylphenyl}methane

To a solution of Boc-L-Arg(Pbf)-OH (0.51 g, 0.97 mmol) in dry DMF (5 mL) were added HOBt (0.15 g, 1.09 mmol) and DCC (0.20 g, 0.96 mmol) and the mixture stirred for 10 minutes. Then compound **7** (0.12 g, 0.29 mmol) dissolved DMF (2 mL) was added. The mixture was stirred at room temperature for 24 h. Ethyl acetate was added (10 mL), DCU was filtered off by gravity on a PTFE filter, and the solvent was removed under reduced pressure. The crude was dissolved in ethyl acetate (10 mL) and washed with a saturated $NaHCO_3$ aqueous solution (10 mL), brine (3×10 mL) and dried over anhydrous Na_2SO_4. The solvent was removed under reduced pressure giving a crude material that was purified by preparative TLC (eluent: AcOEt/hexane= 2:1) to obtain the pure product as a white solid in 10% yield.

Mp: 136-138 °C dec. ^{1}H NMR (300 MHz, CD_3OD) δ 7.70 (bs, 2H, Ar*H*), 6.75 (bs, 2H, Ar*H*),

4.35-3.50 (bm, 8H, ArCH_2Ar, NHCOCH and OCH_2), 3.30-3.02 (bm, 4H, N=CNHCH_2), 2.92 (s, 4H, C$H_{2\ Pbf}$), 2.52 (s, 6H, C$H_{3\ Pbf}$), 2.46 (s, 6H, C$H_{3\ Pbf}$), 2.23 (s, 6H, ArCH_3), 1.99 (s, 6H, CH_{3Pbf}), 1.90-1.10 (m, 54H, N=CNHCH$_2$CH_2CH_2, C(CH_3)$_{3\ Boc}$, C(CH_3)$_{2\ Pbf}$ and OCH$_2$CH_2CH_2CH_2CH_2), 0.90 (bs, 6H, CH$_2$CH_3).

^{13}C NMR (100 MHz, CD$_3$OD) δ 173.5 (*C*=O), 159.8(*C*=N), 158.1(*C*=O), 158.0 (*C* Ar $_{Pbf}$), 153.5 (*C* Ar $_{gemini}$), 139.4 (*C* Ar $_{Pbf}$), 135.1 and 134.8 (*C* Ar $_{gemini}$), 134.3 and 133.5 (*C* Ar $_{Pbf}$), 132.4 (*C* Ar $_{gemini}$), 125.9 (*C* Ar $_{Pbf}$), 122.1 and 121.0 (*C* Ar $_{gemini}$), 118.4 (*C* Ar $_{Pbf}$), 87.6 (*C*(CH$_3$)$_{2\ Pbf}$), 80.8 (*C*(CH$_3$)$_3$), 74.1 (O*C*H$_2$), 56.5 (CO*C*HNHBoc), 44.0 (*C*H$_{2\ Pbf}$), 41.6 (N=CNH*C*H$_2$), 33.0 (OCH$_2$CH$_2$*C*H$_2$), 31.4 (OCH$_2$*C*H$_2$), 30.9 (Ar*C*H$_2$Ar), 30.8 (COCH*C*H$_2$), 28.8 and 28.7 (C(*C*H$_3$)$_2$ and C(*C*H$_3$)$_3$), 27.3 (COCHCH$_2$*C*H$_2$), 27.0 (*C*H$_2$CH$_2$CH$_3$), 23.7 (*C*H$_2$CH$_3$), 19.7 and 18.5 (*C*H$_{3\ Pbf}$), 17.0 (Ar*C*H$_3$), 14.5 (CH$_2$*C*H$_3$), 12.6 (*C*H$_{3\ Pbf}$).

ESI-MS (m/z): [M + Na]$^+$ calcd for $C_{75}H_{114}N_{10}O_{14}$ 1465.8, found 1466.0.

General procedure for Boc/Pbf deprotection:

A solution of calix[4]arene (10 mmol) in TFA/TIS/H$_2$O (95/2.5/2.5, 2 mL) was stirred at room temperature. The progression of the reaction was followed using mass spectroscopy. After completion (1-2 h), the volatiles were removed under reduced pressure and the residue washed with ethyl acetate (3×5 mL) to remove the exceeding TFA. The crude material was precipitated, washed and centrifuged with anhydrous diethyl ether (3×7 mL). The trifluoroacetate anion of the resulting TFA salts was exchanged by adding 10 mM HCl solution (3×5 mL) followed by evaporation under reduced pressure.

Synthesis of 5,11,17,23-Tetra(L-Arg-amino)-25,26,27,28-tetrakis(*n*-hexyloxy)calix[4]arene, octahydrochloride (3)

The pure product was isolated as white solid in quantitative yield.

Mp: 230-232 °C dec. ^{1}H NMR (300 MHz, CD$_3$OD) δ 7.18 (s, 4H, Ar*H*), 6.87 (s, 4H, Ar*H*), 4.47 (d, *J* = 12.9 Hz, 4H, ArCH_{ax}Ar), 4.06 (bs, 4H, COC*H*NH$_3^+$), 3.90 (t, *J* = 7.3 Hz, 8H, OCH_2), 3.40-3.20 (m, 8H, CH_2NH$_3^+$), 3.16 (d, *J* = 12.9 Hz, 4H, ArCH_{eq}Ar), 1.98 (bs, 16H, OCH$_2$CH_2 and COCHCH_2), 1.72 (bs, 8H, COCHCH$_2$CH_2), 1.50-1.20 (m, 24H, O(CH$_2$)$_2$CH_2CH_2CH_2), 0.94 (t, *J* = 6.3 Hz, 12H, CH$_2$CH_3).

^{13}C NMR (75 MHz, CD$_3$OD) δ 167.9 (*C*=O), 158.9 (*C*=N), 155.1, 136.6, 136.5, 133.2, 122.6 and 122.1(*C* Ar), 77.0 (O*C*H$_2$), 54.8 (CO*C*HNH$_3^+$), 42.2 (N=CNH*C*H$_2$), 33.7 (OCH$_2$CH$_2$*C*H$_2$), 32.4 (OCH$_2$*C*H$_2$), 31.8 (Ar*C*H$_2$Ar), 30.2 (COCH*C*H$_2$), 27.6 (*C*H$_2$CH$_2$CH$_3$),

25.9 ($COCHCH_2CH_2$), 24.3 (CH_2CH_3), 14.8 (CH_2CH_3).

ESI-MS (m/z): $[M + 2H - 8HCl]^{++}$ calcd. for $C_{76}H_{132}Cl_8N_{20}O_8$, 723.5; found, 723.7. HRESI-MS (m/z): $[M + 2H - 8HCl]^{++}$ calcd. for $C_{76}H_{132}Cl_8N_{20}O_8$, 723.50283; found, 723.50357.

Bis(5-L-Arg-amino-2-hexyloxy-3-methylphenyl)methane, tetra-hydrochloride (8)

The pure product **8** was obtained as a white solid in 80% yield.

Mp: 238 °C dec. ^{1}H NMR (400 MHz, CD_3OD) δ 7.50 (s, 2H, Ar*H*), 7.05 (s, 2H, Ar*H*), 4.06 (bt, *J* = 5.6 Hz, 2H, $COCHNH_3^+$), 4.03 (s, 2H, $ArCH_2Ar$), 3.74 (t, *J* = 6.4 Hz, 4H, OCH_2), 3.28 (t, *J* = 6.8 Hz, 4H, $N{=}CNHCH_2$), 2.30 (s, 6H, $ArCH_3$), 2.10-1.90 (m, 4H, $COCHCH_2$), 1.82-1.67 (m, 8H, OCH_2CH_2 and $COCHCH_2CH_2$), 1.55-1.42 (m, 4H, $OCH_2CH_2CH_2$), 1.42-1.28 (m, 8H, $O(CH_2)_3CH_2CH_2$), 0.93 (t, *J* = 6.8 Hz, 6H, CH_2CH_3).

^{1}H NMR (400 MHz, D_2O) δ 7.25 (d, *J* = 2.2 Hz, 2H, Ar*H*), 7.09 (d, *J* = 2.2 Hz, 2H, Ar*H*), 4.12 (t, *J* = 8.8 Hz, 2H, $COCHNH_3^+$), 4.03 (s, 2H, $ArCH_2Ar$), 3.73 (t, *J* = 8.4 Hz, 4H, OCH_2), 3.23 (t, *J* = 8.8 Hz, 4H, $N{=}CNHCH_2$), 2.28 (s, 6H, $ArCH_3$), 2.10-1.92 (m, 4H, $COCHCH_2$), 1.80-1.55 (m, 8H, OCH_2CH_2 and $COCHCH_2CH_2$), 1.42-1.10 (m, 12H, $O(CH_2)_2CH_2CH_2CH_2$), 0.84 (t, *J* = 8.8 Hz, 6H, CH_2CH_3).

^{13}C NMR (100 MHz, CD_3OD) δ 167.9 (*C*=O), 158.6, 154.1, 135.5, 134.5, 132.8, 122.4 and 121.5 (*C* Ar), 74.0 (OCH_2), 54.6 ($COCHNH_3^+$), 41.8 ($N{=}CNHCH_2$), 32.9 ($OCH_2CH_2CH_2$), 31.4 (OCH_2CH_2), 30.7 ($ArCH_2Ar$), 29.9 ($COCHCH_2$), 27.0 ($CH_2CH_2CH_3$), 25.5 ($COCHCH_2CH_2$), 23.7 (CH_2CH_3), 16.8 ($ArCH_3$), 14.4 (CH_2CH_3).

ESI-MS (m/z): $[M + 2H - 4HCl]^{++}$ calcd. for $C_{39}H_{70}Cl_4N_{10}O_4$, 370.3, found 370.9. HRESI-MS (m/z): $[M + 2H - 4HCl]^{++}$ calcd. for $C_{39}H_{70}Cl_4N_{10}O_4$, 370.27070, found 370.27153.

General procedure for Boc deprotection:

A solution of calix[4]arene (10 mmol) in DCM/TFA/TES (87.5/10/2.5, 1 mL) was stirred at 0°C. The progression of the reaction was followed using mass spectroscopy. After completion (1-3 h), the volatiles were removed under reduced pressure. The crude material was precipitated, washed and centrifuged with anhydrous diethyl ether (3×5 mL). The trifluoroacetate anion of the resulting TFA salts was exchanged by adding 10 mM HCl solution in MeOH (3×5 mL) followed by evaporation under reduced pressure.

Synthesis of 5,11,17,23-Tetra(L-Lys-amino)-25,26,27,28-tetrakis(*n*-

hexyloxy)calix[4]arene, octahydrochloride (5)

The pure product **5** was isolated as white solid in quantitative yield.

Mp: >215 °C dec. ^{1}H NMR (300 MHz, CD_3OD) δ 7.21 (d, *J* = 2.4 Hz, 4H, Ar*H*), 6.85 (d, *J* = 2.4 Hz, 4H, Ar*H*), 4.47 (d, *J* = 12.9 Hz, 4H, ArCH_{ax}Ar), 4.03 (t, *J* = 6.6 Hz, 4H, COC*H*NH_3^+), 3.92 (t, *J* = 7.5 Hz, 8H, OCH_2), 3.15 (d, *J* = 12.9 Hz, 4H, ArCH_{eq}Ar), 2.97 (t, *J* = 7.5 Hz, 8H, C$H_2NH_3^+$), 2.08-1.83 (m, 16H, OCH_2CH_2 and $COCHCH_2$), 1.82-1.65 (m, 8H, $CH_2CH_2NH_3^+$), 1.63-1.25 (m, 32H, $COCHCH_2CH_2$ and $O(CH_2)_2CH_2CH_2CH_2$), 0.95 (t, 12H, *J* = 6.7 Hz, CH_2CH_3).

^{1}H NMR (300 MHz, D_2O, c = 1 mM) δ 7.30 (d, *J* = 2.4 Hz, 4H, Ar*H*), 6.85 (d, *J* = 2.4 Hz, 4H, Ar*H*), 4.47 (d, *J* = 13.0 Hz, 4H, ArCH_{ax}Ar), 4.12-3.95 (m, 12H, COC*H*NH_3^+ and OCH_2), 3.35 (d, *J* = 13.0 Hz, 4H, ArCH_{eq}Ar), 3.02 (t, *J* = 7.8 Hz, 8H, C$H_2NH_3^+$), 2.12-1.86 (m, 16H, OCH_2CH_2 and $COCHCH_2$), 1.82-1.62 (m, 8H, $CH_2CH_2NH_3^+$), 1.61-1.23 (m, 32H, $COCHCH_2CH_2$ and $O(CH_2)_2CH_2CH_2CH_2$), 0.94 (t, 12H, *J* = 6.9 Hz, CH_2CH_3).

^{13}C NMR (150 MHz, CD_3OD) δ 167.9 (*C*=O), 154.8, 136.3, 133.0, 122.3 and 121.8 (*C* Ar), 76.8 (OCH_2), 54.7 ($COCHNH_3^+$), 40.4 ($CH_2NH_3^+$), 33.5 ($OCH_2CH_2CH_2$), 32.3 (OCH_2CH_2), 32.1 ($ArCH_2Ar$), 31.5 ($COCHCH_2$), 28.2 ($CH_2CH_2NH_3^+$), 27.3 ($CH_2CH_2CH_3$), 24.1 ($COCHCH_2CH_2$), 23.1(CH_2CH_3), 14.6 (CH_2CH_3).

ESI-MS (m/z): $[M + 2H - 8HCl]^{++}$ calcd. for $C_{76}H_{132}Cl_8N_{12}O_8$, 667.5, found 667.6. HRESI-MS (m/z): $[M + 3H - 8HCl]^{3+}$ calcd. for $C_{76}H_{132}Cl_8N_{12}O_8$, 445.3294; found, 445.3293.

Synthesis of 25,26,27,28-Tetrakis[3-(L-Arg-amino)propoxy]calix[4]arene, octahydrochloride (11)

Calix[4]arene **10** (80 mg, 4.1×10^{-2} mmol) was dissolved in MeOH (13 mL) and a catalytic amount of Pd/C (10%) was added. Hydrogenation for Cbz group removal was carried out at 2 atm in a Parr reactor for 27 h. The reaction was quenched by catalyst filtration and the solvent removed under reduced pressure. Crude was dissolved in 10 mL water, filtered on a Nylon 0.45 mm filter and purified by HPLC (column: Jupiter 4u Proteo 90A, C-12, 90A, 10 mm × 250 mm, elution conditions: eluent A H_2O + 0.1% formic acid; eluent B: MeOH + 0.1% formic acid; 100% A over 5 min, 100% A to 84/16 A/B over 5 min, 84/16 to 74/26 A/B over 20 min, at 4 mL/min; retention time: 15.4 min). The fractions containing the pure product were collected and evaporated under reduced pressure. The formate anion of the resulting salt was exchanged by adding HCl 37% to a methanol solution (5 mL) of the solid

residue till pH 3 followed by evaporation under reduced pressure (4×) and liophilization, to give **11** as white powder (65% yield).

Mp: 182-185 °C. ^{1}H NMR (400 MHz, CD_3OD) δ 8.70 (bt, N*H*CO), 6.63 (d, *J* = 6.6 Hz, 8H, Ar*H*), 6.57 (t, *J* = 6.6 Hz, 4H, Ar*H*), 4.44 (d, *J* = 13.4 Hz, 4H, ArC*H*$_2$Ar), 4.08 (t, *J* = 6.4 Hz, 4H, COC*H*NH), 4.02 (t, *J* = 6.4 Hz, 8H, OC*H*$_2$), 3.52 (t, *J* = 6.8 Hz, 8H, $OCH_2CH_2CH_2$), 3.30 (t, *J* = 5.1 Hz, 8H, C*H*$_2$NHCNH), 3.21 (d, *J* = 13.4 Hz, 4H, ArC*H*$_2$Ar), 2.33-2.12 (m, 8H, OCH_2CH_2), 2.06-1.85 (m, 8H, COCHC*H*$_2$), 1.81-1.63 (m, 8H, $COCHCH_2CH_2$).

^{1}H NMR (300 MHz, D_2O, c = 2.4 mM) δ 6.84 (d, *J* = 7.4 Hz, 8H, Ar*H*), 6.72 (t, *J* = 7.4 Hz, 4H, Ar*H*), 4.41 (d, *J* = 13.2 Hz, 4H, ArC*H*$_{ax}$Ar), 4.14-3.90 (m, 12H, COC*H*NH and OC*H*$_2$), 3.72-3.55 (m, 4H, OCH_2CH_2CHH), 3.46-3.30 (m, 4H, OCH_2CH_2CHH), 3.35 (d, *J* = 13.2 Hz, 4H, ArC*H*$_{eq}$Ar), 3.19 (t, *J* = 6.9 Hz, 8H, C*H*$_2$NHCNH), 2.36-2.10 (m, 8H, OCH_2CH_2), 1.96-1.80 (m, 8H, COCHC*H*$_2$), 1.70-1.52 (m, 8H, $COCHCH_2CH_2$).

^{13}C NMR (100 MHz, CD_3OD) δ 170.1 (*C*=O), 158.6 (*C*=N), 157.5, 136.1, 129.5 and 123.4 (*C* Ar), 73.9 (O*C*H$_2$), 54.1 (CO*C*HNH$_3^+$), 41.9 (N=CNH*C*H$_2$), 38.4 (*C*H$_2$NH), 32.0 (Ar*C*H$_2$Ar), 31.2 (OCH_2CH_2), 29.9 (COCH*C*H$_2$), 25.6 (COCH CH_2CH_2).

ESI-MS (m/z): $[M + 2H - 8HCl]^{++}$ calcd. for $C_{64}H_{108}Cl_8N_{20}O_8$, 639.4, found 639.9. HRMS (m/z): $[M + 2H - 8HCl]^{++}$ calcd. for $C_{64}H_{108}Cl_8N_{20}O_8$, 639.40893, found 639.40911.

DNA preparation and storage. Plasmid DNA (pEGFP-C1) was purified through cesium chloride gradient centrifugation (Maniatis, T., Fritsch, E. F., and Sambrook, J. (1989) *Molecular Cloning: A Laboratory Manual* Cold Spring Harbor Laboratory, New York). A stock solution of the plasmid 0.35 mM in milliQ water (Millipore Corp., Burlington, MA) was stored at -20 °C.

Fluorescence studies. Ethidium Bromide Displacement Assays (excitation at 530 nm, emission at 600 nm) were performed collecting on a PerkinElmer LS 55 the emission spectra of buffer solutions (4 mM Hepes, 10 mM NaCl, pH 7.4) of 50 mM ethidium bromide (relative fluorescence = 0), mixture of 0.5 nM plasmid DNA (pEGFP-C1) and 50 mM ethidium bromide (relative fluorescence = 1) and after addition of increasing amounts of ligand. Experiments with Nile Red were performed on the same instrument (excitation at 530 nm) in buffer solutions (4 mM Hepes, 10 mM NaCl, 2 mM $MgCl_2$, pH = 7.4) of the dye (0.2 mM) and mixture of the dye with ligand (2 mM) and pEGFP-C1 DNA (0.5 nM).

Electrophoresis mobility shift assay (EMSA). Binding reactions were performed in a final volume of 14 mL with 10 mL of 20 mM Tris/HCl pH 8, 1 mL of plasmid (1 mg of pEGFP-C1) and 3 mL of compound at different final concentrations, ranging from 25 to 200 mM. Binding reaction was left to take place at room temperature for 1 h; 5 mL of 1 g/mL in H_2O of glycerol was added to each reaction mixture and loaded on a TA (40 mM Tris-Acetate) 1% agarose gel. At the end of the binding reaction 1 mL (0.01 mg) of ethidium bromide solution is added. The gel was run for 2.5 h in TA buffer at 10 V/cm. EDTA was omitted from the buffers because it competes with DNA in the reaction.

Sample preparation and AFM imaging. DNA samples were prepared by diluting the plasmid DNA to a final concentration of 0.5 nM in deposition buffer (4 mM Hepes, 10 mM NaCl, 2 mM $MgCl_2$, pH = 7.4) either in the presence or absence of ligands. When needed, ethanol at a defined concentration was added to the deposition buffer prior to addition of DNA and calixarenes. The mixture was incubated for 5 min at room temperature, then a 20 mL droplet was deposited onto freshly-cleaved ruby mica (Ted Pella, Redding, CA) for 1.5 min. The mica disk was rinsed with milliQ water and dried with a weak nitrogen stream. AFM imaging was performed on the dried sample with a Nanoscope IIIA Microscope (Digital Instruments Inc. Santa Barbara, CA) operating in tapping mode. Commercial diving board silicon cantilevers (NSC-15 Micromash Corp., Estonia) were used. Images of 512×512 pixels were collected with a scan size of 2 mm at a scan rate of 3-4 lines per second and were flattened after recording using Nanoscope software.

Measurement of the Size of the Complexes by Dynamic Light Scattering (DLS) and of the ζ-Potential. The average sizes of the calix-pDNA complexes were measured using a Zetasizer nano with the following specification: sampling time, automatic; number of measurements, 3 per sample; medium viscosity, 1.054 cP; refractive index, 1.33; scattering angle, 173°; λ = 633 nm; temperature, 25°C. Data were analyzed using the

multimodal number distribution software included in the instrument. Results are given as volume distribution of the major population by the mean diameter with its standard deviation. Zeta-potential measurements were made using the same apparatus with "mixed-mode measurement" phase analysis light scattering (M3-PALS). M3-PALS consists of both slow field reversal and fast field reversal measurements, hence the name "mixed-mode measurement"; it improves accuracy and resolution. The following specifications were applied: sampling time, automatic; number of measurements, 3 per sample; medium viscosity, 1.054 cP; medium dielectric constant, 80; temperature, 25°C. Before each series of experiments, the performance of the instruments was checked with either a 90 nm monodisperse latex beads (Coulter) for DLS or with DTS 50 standard solution (Malvern) for ζ potentials.

Transmission Electron Microscopy (TEM). Formvar-carboncoated grids were placed on top of small drops of the calix-pDNA complex (HEPES 20 mM, pH 7.4, DNA 60 µM phosphate). After 1-3 min of contact, grids were negatively stained with a few drops of 1% aqueous solution of uranyl acetate. The grids were then dried and observed using an electron microscope working under standard conditions.

Cell culture and transient transfection assay. RD-4 [human Rhabdomyosarcoma cell line (obtained from David Derse, National Cancer Institute, Frederick, Maryland)], C2C12 [mouse myoblast; ATCC (#CRL-1772)], N2a [mouse neuroblastoma; ATCC (#CCL-131)], EADSc [Equine Adipose Derived Stromal Cells primary culture was obtained as described in Donofrio, G. et al. *Cell Biology* **2010**, *11*, 73], COS-7 [African Green Monkey Kidney cells; ATCC (#CRL-1651)], VERO [African Green Monkey Kidney Cells; ATCC (#CCL-81), HEK 293 [Human embryo Kidney cells; ATCC (#CRL-1573)], Ishikawa [Human Endometrial cancer cells; ECACC (#99040201)] and HeLa [Human Cervix Adenocarcinoma; ATCC (#CCL-2)] were grown in EMEM medium containing NEAA, 10% FBS, 2 mM l-glutamine, 100 IU/mL penicillin and 100 mg/mL streptomycin. All cultures were incubated at 37 °C in a humidified atmosphere containing 5% CO_2. Cells were subcultured to a fresh culture vessel when growth reached 70-90% confluence (i.e. every 3-5 days) and incubated at 37 °C in a humidified atmosphere of 95% air-5% CO_2. Transfections were performed in 24 well plates, when cells were 80% confluent (approximately 5×10^4 cells) on the day of transfection. 2.5 mg of plasmid and different

concentrations of ligands were added to 1 mL of serum-free medium (DMEM, 2 mM L-glutamine and 50 µg/ml), mixed rapidly and incubated at room temperature for 20 min. When used, serum was added at this point to the transfection solution. Following the removal of the culture medium from the cells, 0.5 mL of transfection mixture were carefully added to every well. Lipoplex formulations with helper lipid were prepared adding a 2 mM ethanol solution of DOPE to plasmid-ligand mixture at 1:2 ligand:DOPE molar ratio, where ligand concentration was kept to 10 mM. These solutions administered to the cells were completely clear and homogeneus. LTX™ transfection reagent was used according to manufacturer's protocol as positive transfection control. The mixture and cells were incubated at 37 °C in a humidified atmosphere of 95% air-5% CO_2 for 5 h. Finally, transfection mixture was removed and 1 mL of growth medium added to each transfected well and left to incubate for 72 h. Five fields were randomly selected from each well without viewing the cells (one in the centre and one for each quadrant of the well) and examined. The transfected cells were observed under fluorescence microscope for EGFP expression. Each experiment was done three times. Statistical differences between treatments were calculated with Student's test and multifactorial ANOVA.

Luciferase reporter assay. Luciferase reporter assay was performed with a Dual Luciferase Reporter Assay System kit (Promega) with minor modifications. Following treatments, cells were washed with PBS, lysed with 100 μl of lysis passive buffer by freeze-thawing at −80 °C. 10 μl of the cell lysate was added to 50 μl of LAR and Luciferase activity were determined with a PerkinElmer Victor Multilabel Counter, according to the manufacturer's specifications. Individual assays were normalized for *Renilla* Luciferase activity with a second reading, adding 50 ml of Stop & Glo substrate.

MTT survival assay for cell viability determination. 2000 cells/well (in 50 µL) were seeded in a 96 wells plate, cells were grown in complete medium (90% DMEM, 10% FBS, 2 mM L-glutamine, and 100 IU/mL penicillin, 10 mg/mL streptomycin) and incubated at 37°C overnight. The day after 50 µL of scalar dilution of calixarenes, alone or with DOPE, were added to the cells and incubated at 37°C overnight. Calixarenes were tested from 40 to 2.5 µM and DOPE from 80 to 5 µM. 24 hours later, 10 µL of complete medium containing MTT (5 mg/mL) was added to each well and incubated for 6 h. Then, after the addition of 100 µL per well of solubilisation solution (10% SDS in HCl 0.01 M) cells were

incubated at 37 °C overnight. MTT survival assay for cell viability determination in transfection conditions was performed with the same procedure at 24 h from transfection (see transient transfection assay). Specific optical density for each well was measured at 540 nm, using 690 nm as reference wavelength in an SLT-Lab microreader (Salzburg, Austria). Each experiment was done three times and each treatment was performed with eight replicates. Statistical differences among treatments were calculated with Student's test and multifactorial ANOVA.

2.5 References

[1] *Cell-Penetrating Peptides. Methods and Protocols*; Langel, Ed.; Humana Press: New York, **2011**.

[2] a) Brasseur, R.; Divita, G. *Biochim. Biophys. Acta* **2010**, *1798*, 2177–2181; b) Heitz, F.; Morris, M.C.; Divita, G. *J. Pharmacol*. **2009**, *157*, 195–206.

[3] a) Frankel, A.D. and Pabo, C.O. *Cell* **1988**, *55*, 1189–1193; b) Vives, E., Brodin, P. and Lebleu, B. *J. Biol. Chem.* **1997**, *272*, 16010–16017.

[4] a) Torchilin, V., Rammohan, R., Weissig, V. and Levchenko, T. *Proc. Natl. Acad. Sci*. **2001**, *98*, 8786–8791; b) Kleemann, E.; Neu, M.; Jekel, N.; Fink, L.; Schmehl, T.; Gessler, T.; Seeger, W.; Kissel, T. *J. Control. Release* **2005**, *109*, 299–316.

[5] Futaki, S.; Suzuki, T.; Ohashi, W.; Yagami, T.; Tanaka, S.; Ueda, K.; Sugiura, Y. *J. Biol. Chem.* **2001**, *276*, 5836–5840.

[6] a) Rothbard, J.B.; Garlington, S.; Lin, Q.; Kirschberg, T.; Kreider, E.; McGrane, P.L.; Wender, P.A.; Khavari, P.A. *Nat. Med.* **2000**, *6*, 1253–1257; b) S. Futaki, *Biopolymers* **2006**, *84*, 241–249.

[7] Said Hassane, F.; Saleh, A. F.; Abes, R.; Gait, M. J.; Lebleu, B. *Cell. Mol. Life Sci*. **2010**, *67*, 715–726.

[8] a) Mann, A.; Thakur, G.; Shukla, V.; Singh, A. K.; Khanduri, R.; Naik, R.; Jiang, Y.; Kalra, N.; Dwarakanath, B. S.; Langel, Ganguli, M. *Mol. Pharmaceutics* **2011**, *8*, 1729–1741; b) Mitchell, D.J., Kim, D.T., Steinman, L., Fathman, C.G.; Rothbard, J.B. *J. Pept. Res.* **2000**, *56*, 318–325.

[9] Rothbard, J.B.; Jessop, T.C.; Lewis, R.S.; Murray, B.A.; Wender, P.A. *J. Am. Chem. Soc.* **2004**, *126*, 9506–9507.

[10] a) Khalil, I. A.; Kogure, K.; Futaki, S.; Harashima, H. *Int. J. Pharm*. **2008**, *354*, 39–48.

[11] a) Futaki, S.; Ohashi, W.; Suzuki, T.; Niwa, M.; Tanaka, S.; Ueda, K.; Harashima, H.; Sugiura, Y. *Bioconjugate Chem.* **2001**, *12*, 1005–1011; b) Khalil, I. A.; Futaki, S.; Niwa,M.; Baba, Y.; Kaji, N.; Kamiya, H.; Harashima, H. *Gene Ther*. **2004**, *11*, 636–644.

[12] a) Khalil, I. A.; Kogure, K.; Futaki, S.; Hama, S.; Akita, H.; Ueno, M.; Kishida, H.; Kudoh, M.; Mishina, Y.; Kataoka, K.; Yamada, M.; Harashima, H. *Gene Ther*. **2007**, *14*, 682–689; b) Nakamura, Y.; Kogure, K.; Futaki, S.; Harashima, H. *J. Controlled Release* **2007**, *119*, 360– 367.

[13] Kogure, K.; Akita, H.; Yamada, Y.; Harashima, H. *Adv. Drug Delivery Rev.* **2008**, *60*, 559–571.

[14] a) Akita, H.; Kudo, A.; Minoura, A.; Yamaguti, M.; Khalil, I. A.; Moriguchi, R.; Masuda, T.; Danev, R.; Nagayama, K.; Kogure, K.; Harashima, H. *Biomaterials* **2009**, *30*, 2940–2949; b) R. Moriguchi, K. Kogure, H. Akita, S. Futaki, M. Miyagishi, K. Taira, H. Harashima, *Int. J. Pharm.* **2005**, *301*, 277–285.

[15] Mäe, M.; El Andaloussi, S.; Lundin, P.; Oskolkov, N.; Johansson, H. J.; Guterstam, P.; Langel, *J. Controlled Release* **2009**, *134*, 221–227.

[16] El Andaloussi, S.; Lehto, T.; Mäger, I.; Rosenthal-Aizman, K.; Oprea, I. I.; Simonson, O. E.; Sork, H.; Ezzat, K.; Copolovici, D. M.; Kurrikoff, K.; Viola, J. R.; Zaghloul, E. M.; Sillard, R.; Johansson, H. J.; Said Hassane, F.; Guterstam, P.; Suhorutsenko, J.; Moreno, P. M.; Oskolkov, N.; Hälldin, J.; Tedebark, U.; Metspalu, A.; Lebleu, B.; Lehtieo, J.; Smith, C. I.; Langel, *Nucleic Acids Res.* **2011**, *39*, 3972–3987.

[17] Alexis, F.; Lo, S.L.; Wang, S. *Adv. Mater.* **2006**, *18*, 2174–2178.

[18] Wender, P.A., Mitchell, D.J., Pattabiraman, K., Pelkey, E.T., Steinman, L. and Rothbard, J.B. *Proc. Natl. Acad. Sci.* **2000**, *97*, 13003–13008.

[19] Wender, P., Rothbard, J., Jessop, T., Kreider, E. and Wylie, B. *J. Am. Chem. Soc.* **2002**, *124*, 13382–13383.

[20] Wender, P., Kreider, E., Pelkey, E., Rothbard, J. and VanDeusen, C. *Org. Lett.* **2005**, *7*, 4815– 4818.

[21] a) Deglane, G.; Abes, S.; Michel, T.; Prevot, P.; Vives, E.; Debart, F.; Barvik, I.; Lebleu, B.; Vasseur, J.J. *Chembiochem* **2006**, *7*, 684–692; b) Dragulescu-Andrasi, A.; Rapireddy, S.; He, G.; Bhattacharya, B.; Hyldig- Nielsen, J.J.; Zon, G.; Ly, D.H. *J. Am. Chem. Soc.* **2006**, *128*, 16104–16112; c) Zhou, P.; Wang, M.; Du, L.; Fisher, G.W.; Waggoner, A.; Ly, D.H. *J. Am. Chem. Soc.* **2003**, *125*, 6878–6879.

[22] Baldini, L.; Sansone, F.; Scaravelli, F.; Massera, C.; Casnati, A.; Ungaro, R. *Tetrahedron letters* **2009,** *50,* 3450-3453.

[23] Smukste, I.; House, B. E.; Smithrud, D. B. *J. Org. Chem.* **2003,** *68,* 2559-2571.

[24] Bogan, A. S.; Thorn, K. S. *J. Mol. Biol.* **1998,** *280,* 1-9.

[25] Martos, V.; Bell, S. C.; Santos, E.; Isacoff, E. Y.; Trauner, D.; de Mendoza, J. *PNAS* **2009,** *106,* 10482-10486.

[26] a) Sansone, F.; Dudic, M.; Donofrio, G.; Rivetti, C.; Baldini, L.; Casnati, A.; Cellai, S.; Ungaro, R. *J. Am. Chem. Soc.* **2006**, *128*, 14528-14536; b) Bagnacani, V., Sansone, F., Donofrio, G., Baldini, L., Casnati, A., Ungaro, R. *Org. Lett*. **2008**, *10*, 3953−3956; c) Bagnacani, V., Franceschi, V.; Fantuzzi, L.; Casnati, A., Donofrio, G., Sansone, F., Ungaro, R. *Bioconjugate Chem*. **2012**, *23*, 993−1002.

[27] El-Sayed, A.; Khalil, I. A.; Kogure, K.; Futaki, S.; Harashima, H. *J. Biol. Chem.* **2008**, *283*, 23450–23461.

[28] Bagnacani, V. Ph.D. Thesis "Synthetic ligands in bio-organic chemistry: guanidinium-mediated ion transport and gene delivery and development of a β-sheet propensity scale", **2010**.

[29] Radau, G. *Monatshefte fur Chemie* **2003**, *134*, 1033-1036.

[30] Della Ca', N.; Fontanella, M.; Sansone, F.; Ugozzoli, F.; Ungaro, R.; Liger, K; Dozol, J.-F. *Eur. J Org. Chem.* **2005**, *11*, 2338-2348.

[31] Sun, P.; Lu, H.; Yao, X.; Tu, X.; Zheng, Z.; Wang, X. J. Mater. Chem., **2012**, *22*, 10035-10041.